acid substitutions stabilized the α-helix of C-HR peptides and increased their binding affinity to N-HR, thus providing potent anti-HIV activity. This property may be one of the key attributes of the recently developed potent peptide inhibitors, SC34EK (6, 30), T-20EK (31), or T-2429 (5), that have been reported to efficiently inhibit T-20 resistant variants. However, the S138A substitution on T-20 in the present study had little effect on the random coil structure, as judged by CD (data not shown), indicating that $T\text{-}20_{S138A}$ increases its binding affinity not by simply enhancing the α-helicity of this region (5, 6). Our approach of introducing substitutions selected on the basis of the mutation(s) that appears in resistant viruses significantly improved the affinity with N-HR. This approach may complement the effects of enhancing helical stability and may help generate more potent and effective fusion inhibitors for resistant HIV-1 variants.

Other methods have also been employed to improve the potency of HIV fusion inhibitors. For example, T-1249 is a peptide that is based on the T-20 sequence and has improved binding properties (32, 33). It contains 17 changes compared with T-20 (3 additional residues and 14 substitutions to increase the α-helicity/binding affinity according to amino acid sequences of HIV-2 and simian immunodeficiency virus). T-2635 is another efficient peptide fusion inhibitor that was recently developed and is also modified extensively (19 substitutions in 38 amino acids) (5). Also, SC34EK is an electrostatically constrained peptide that also suppresses replication of T-20-resistant variants, and it required 12 substitutions in the original C34 inhibitor (6, 30). Hence, it is possible to improve the potency of existing peptide inhibitors through intense modeling and iterative testing in *in vitro* studies that could lead to the design and synthesis of improved peptide drugs. However, the approach we followed in the design of the $T\text{-}20_{S138A}$ inhibitor is considerably simpler and involves a smaller number of sequence changes (1 residue changed, compared with 19 and 12 in the cases of T-2635 and SC34EK, respectively; see above). It takes advantage of information obtained from the viral evolution under drug pressure and uses the resistance information to design improved inhibitors. In addition, we believe that this approach may be applicable to other targets even when the interactions do not involve helical bundles or detailed information on related systems is not available. Importantly, whenever possible, a combination of the two approaches would likely generate even more effective peptide inhibitors that can suppress replication of resistant variants.

α-Helical structure is a significant factor not only in HIV-1 fusion but also in other examples of protein-protein interactions. Peptide-based drugs have to overcome multiple obstacles, including poor oral bioavailability, less permeability into the target cells, and high cost. Several modifications, such as using arginine-rich peptide tags (34, 35), and chemical treatments (36) have been used to overcome the cell permeability problem. At any rate, peptide-based reagents can be an important tool in the discovery and validation of novel therapeutic targets through *in vitro* experiments. For example, it has been shown that the function of a target protein can be inhibited by designing synthetic peptides that have the amino acid sequence of a domain which is important for the protein function. In such cases the peptides may act as decoys that have antagonistic/agonistic or competitive effects, leading to inhibition of the protein function. Similarly, screening through peptide sequences of proteins may be useful for the identification of functionally important domains that could become future targets for peptide-based or small molecule-based drug development.

In this study we designed peptides tailored to suppress T-20-resistant HIV-1 strains. To our knowledge, this is the first report of direct application of resistance information in drug design and may be applicable to other, unrelated systems. For example, a BH3 domain of the anti-apoptotic protein Bcl-2 has been targeted by an α-helical domain mimic peptide (37, 38). The resulting hydrocarbon-stapled peptide, $SAHB_{A,}$ penetrates into cells via endocytosis pathway and inhibits the function of Bcl-2, inducing apoptosis in transplanted leukemia cells in mice. However, during prolonged therapy with such peptides, leukemic cells could develop resistance to the peptides through substitutions in the Bcl-2 region in the selection process for survival reminiscent of HIV-1. One can envision that our strategy of using mutational resistance information to overcome drug resistance might help in the design of substituted peptides that suppress the resistant variants more efficiently, thus contributing to broader applications of successful peptide-based therapies.

REFERENCES

1. Chan, D. C., and Kim, P. S. (1998) *Cell* **93,** 681–684
2. Weiss, C. D. (2003) *AIDS Rev.* **5,** 214–221
3. Jiang, S., Lin, K., Strick, N., and Neurath, A. R. (1993) *Nature* **365,** 113
4. Chan, D. C., Chutkowski, C. T., and Kim, P. S. (1998) *Proc. Natl. Acad. Sci. U. S. A.* **95,** 15613–15617
5. Dwyer, J. J., Wilson, K. L., Davison, D. K., Freel, S. A., Seedorff, J. E., Wring, S. A., Tvermoes, N. A., Matthews, T. J., Greenberg, M. L., and Delmedico, M. K. (2007) *Proc. Natl. Acad. Sci. U. S. A.* **104,** 12772–12777
6. Otaka, A., Nakamura, M., Nameki, D., Kodama, E., Uchiyama, S., Nakamura, S., Nakano, H., Tamamura, H., Kobayashi, Y., Matsuoka, M., and Fujii, N. (2002) *Angew. Chem. Int. Ed. Engl.* **41,** 2937–2940
7. Lalezari, J. P., Henry, K., O'Hearn, M., Montaner, J. S., Piliero, P. J., Trottier, B., Walmsley, S., Cohen, C., Kuritzkes, D. R., Eron, J. J., Jr., Chung, J., DeMasi, R., Donatacci, L., Drobnes, C., Delehanty, J., and Salgo, M. (2003) *N. Engl. J. Med.* **348,** 2175–2185
8. Lazzarin, A., Clotet, B., Cooper, D., Reynes, J., Arasteh, K., Nelson, M., Katlama, C., Stellbrink, H. J., Delfraissy, J. F., Lange, J., Huson, L., DeMasi, R., Wat, C., Delehanty, J., Drobnes, C., and Salgo, M. (2003) *N. Engl. J. Med.* **348,** 2186–2195
9. Baldwin, C. E., and Berkhout, B. (2006) *Retrovirology* **3,** 84
10. Cabrera, C., Marfil, S., Garcia, E., Martinez-Picado, J., Bonjoch, A., Bofill, M., Moreno, S., Ribera, E., Domingo, P., Clotet, B., and Ruiz, L. (2006) *AIDS* **20,** 2075–2080
11. Labrosse, B., Morand-Joubert, L., Goubard, A., Rochas, S., Labernardiere, J. L., Pacanowski, J., Meynard, J. L., Hance, A. J., Clavel, F., and Mammano, F. (2006) *J. Virol.* **80,** 8807–8819
12. Mink, M., Mosier, S. M., Janumpalli, S., Davison, D., Jin, L., Melby, T., Sista, P., Erickson, J., Lambert, D., Stanfield-Oakley, S. A., Salgo, M., Cammack, N., Matthews, T., and Greenberg, M. L. (2005) *J. Virol.* **79,** 12447–12454
13. Nameki, D., Kodama, E., Ikeuchi, M., Mabuchi, N., Otaka, A., Tamamura, H., Ohno, M., Fujii, N., and Matsuoka, M. (2005) *J. Virol.* **79,** 764–770
14. Perez-Alvarez, L., Carmona, R., Ocampo, A., Asorey, A., Miralles, C., Perez de Castro, S., Pinilla, M., Contreras, G., Taboada, J. A., and Najera, R. (2006) *J. Med. Virol.* **78,** 141–147
15. Xu, L., Pozniak, A., Wildfire, A., Stanfield-Oakley, S. A., Mosier, S. M., Ratcliffe, D., Workman, J., Joall, A., Myers, R., Smit, E., Cane, P. A., Greenberg, M. L., and Pillay, D. (2005) *Antimicrob. Agents Chemother.* **49,**

1113–1119
16. Armand-Ugon, M., Gutierrez, A., Clotet, B., and Este, J. A. (2003) *Antiviral Res.* **59,** 137–142
17. Baldwin, C. E., Sanders, R. W., Deng, Y., Jurriaans, S., Lange, J. M., Lu, M., and Berkhout, B. (2004) *J. Virol.* **78,** 12428–12437
18. Baldwin, C., and Berkhout, B. (2008) *J. Virol.* **82,** 7735–7740
19. Kimpton, J., and Emerman, M. (1992) *J. Virol.* **66,** 2232–2239
20. Maeda, Y., Venzon, D. J., and Mitsuya, H. (1998) *J. Infect. Dis.* **177,** 1207–1213
21. Adachi, A., Gendelman, H. E., Koenig, S., Folks, T., Willey, R., Rabson, A., and Martin, M. A. (1986) *J. Virol.* **59,** 284–291
22. Hachiya, A., Kodama, E. N., Sarafianos, S. G., Schuckmann, M. M., Sakagami, Y., Matsuoka, M., Takiguchi, M., Gatanaga, H., and Oka, S. (2008) *J. Virol.* **82,** 3261–3270
23. Chan, D. C., Fass, D., Berger, J. M., and Kim, P. S. (1997) *Cell* **89,** 263–273
24. Case, D. A., Cheatham, T. E., 3rd, Darden, T., Gohlke, H., Luo, R., Merz, K. M., Jr., Onufriev, A., Simmerling, C., Wang, B., and Woods, R. J. (2005) *J. Comput. Chem.* **26,** 1668–1688
25. Nilsson, I., Saaf, A., Whitley, P., Gafvelin, G., Waller, C., and von Heijne, G. (1998) *J. Mol. Biol.* **284,** 1165–1175
26. Eckert, D. M., and Kim, P. S. (2001) *Annu. Rev. Biochem.* **70,** 777–810
27. Bai, X., Wilson, K. L., Seedorff, J. E., Ahrens, D., Green, J., Davison, D. K., Jin, L., Stanfield-Oakley, S. A., Mosier, S. M., Melby, T. E., Cammack, N., Wang, Z., Greenberg, M. L., and Dwyer, J. J. (2008) *Biochemistry* **47,** 6662–6670
28. Watabe, T., Oishi, S., Watanabe, K., Ohno, H., Nakano, H., Nakatsu, T., Kato, H., Izumi, K., Kodama, E., Matsuoka, M., and Fujii, N. (2009) *Peptide Science*, in press
29. Nishitsuji, H., Kohara, M., Kannagi, M., and Masuda, T. (2006) *J. Virol.* **80,** 7658–7666
30. Nishikawa, H., Nakamura, S., Kodama, E., Ito, S., Kajiwara, K., Izumi, K., Sakagami, Y., Oishi, S., Ohkubo, T., Kobayashi, Y., Otaka, A., Fujii, N., and Matsuoka, M. (September 10, 2008) *Int. J. Biochem. Cell Biol.* 10.1016/j.biocel.2008.08.039
31. Oishi, S., Ito, S., Nishikawa, H., Watanabe, K., Tanaka, M., Ohno, H., Izumi, K., Sakagami, Y., Kodama, E., Matsuoka, M., and Fujii, N. (2008) *J. Med. Chem.* **51,** 388–391
32. Chinnadurai, R., Rajan, D., Munch, J., and Kirchhoff, F. (2007) *J. Virol.* **81,** 6563–6572
33. Eggink, D., Baldwin, C. E., Deng, Y., Langedijk, J. P., Lu, M., Sanders, R. W., and Berkhout, B. (2008) *J. Virol.* **82,** 6678–6688
34. Futaki, S., Suzuki, T., Ohashi, W., Yagami, T., Tanaka, S., Ueda, K., and Sugiura, Y. (2001) *J. Biol. Chem.* **276,** 5836–5840
35. Nagahara, H., Vocero-Akbani, A. M., Snyder, E. L., Ho, A., Latham, D. G., Lissy, N. A., Becker-Hapak, M., Ezhevsky, S. A., and Dowdy, S. F. (1998) *Nat. Med.* **4,** 1449–1452
36. Takeuchi, T., Kosuge, M., Tadokoro, A., Sugiura, Y., Nishi, M., Kawata, M., Sakai, N., Matile, S., and Futaki, S. (2006) *ACS Chem. Biol.* **1,** 299–303
37. Walensky, L. D., Kung, A. L., Escher, I., Malia, T. J., Barbuto, S., Wright, R. D., Wagner, G., Verdine, G. L., and Korsmeyer, S. J. (2004) *Science* **305,** 1466–1470
38. Walensky, L. D., Pitter, K., Morash, J., Oh, K. J., Barbuto, S., Fisher, J., Smith, E., Verdine, G. L., and Korsmeyer, S. J. (2006) *Mol. Cell* **24,** 199–210

ANTIMICROBIAL AGENTS AND CHEMOTHERAPY, Mar. 2009, p. 1013–1018 Vol. 53, No. 3
0066-4804/09/$08.00+0 doi:10.1128/AAC.01211-08

SC29EK, a Peptide Fusion Inhibitor with Enhanced α-Helicity, Inhibits Replication of Human Immunodeficiency Virus Type 1 Mutants Resistant to Enfuvirtide[▽]

Takeshi Naito,[1] Kazuki Izumi,[1] Eiichi Kodama,[1]* Yasuko Sakagami,[1] Keiko Kajiwara,[1] Hiroki Nishikawa,[2] Kentaro Watanabe,[2] Stefan G. Sarafianos,[3] Shinya Oishi,[2] Nobutaka Fujii,[2] and Masao Matsuoka[1]

Laboratory of Virus Control, Institute for Virus Research, Kyoto University, 53 Kawaramachi, Shogoin, Sakyo-ku, Kyoto 606-8507, Japan[1]; Graduate School of Pharmaceutical Sciences, Kyoto University, Sakyo-ku, Kyoto 606-8501, Japan[2]; and Department of Molecular Microbiology and Immunology, University of Missouri School of Medicine, Columbia, Missouri[3]

Received 12 September 2008/Returned for modification 24 October 2008/Accepted 23 December 2008

Peptides derived from the α-helical domains of human immunodeficiency virus (HIV) type 1 (HIV-1) gp41 inhibit HIV-1 fusion to the cell membrane. Enfuvirtide (T-20) is a peptide-based drug that targets the step of HIV fusion, and as such, it effectively suppresses the replication of HIV-1 strains that are either wild type or resistant to multiple reverse transcriptase and/or protease inhibitors. However, HIV-1 variants with T-20 resistance have emerged; therefore, the development of new and potent inhibitors is urgently needed. We have developed a novel HIV fusion inhibitor, SC34EK, which is a gp41-derived 34-amino-acid peptide with glutamate (E) and lysine (K) substitutions on its solvent-accessible site that stabilize its α-helicity. Importantly, SC34EK effectively inhibits the replication of T-20-resistant HIV-1 strains as well as wild-type HIV-1. In this report, we introduce SC29EK, a 29-amino-acid peptide that is a shorter variant of SC34EK. SC29EK blocked the replication of T-20-resistant HIV-1 strains and maintained antiviral activity even in the presence of high serum concentrations (up to 50%). Circular dichroism analysis revealed that the α-helicity of SC29EK was well maintained, while that of the parental peptide, C29, which showed moderate and reduced inhibition of wild-type and T-20-resistant HIV-1 strains, was lower. Our results show that the α-helicity in a peptide-based fusion inhibitor is a key factor for activity and enables the design of short peptide inhibitors with improved pharmacological properties.

The envelope proteins of human immunodeficiency virus (HIV) type 1 (HIV-1) exist as functional trimeric complexes of gp120-gp41 heterodimers and play an important role in viral entry into host cells. Interactions of gp120 with CD4 molecules expressed on the cell surface cause structural changes that allow further interactions with the CXCR4 or CCR5 coreceptor. These interactions also induce a conformational change in gp120 that initiates gp41-mediated membrane fusion that leads to viral entry (4). In the process of fusion, the amino-terminal heptad repeat (N-HR) of gp41 trimer interacts with the carboxyl-terminal heptad repeat (C-HR) of gp41 trimer to form a six-helix bundle that makes viral and cell membranes accessible (3).

Peptides derived from N-HR or C-HR, such as N36 (3, 18) and enfuvirtide (T-20) (30), suppress the six-helix bundle formation, resulting in the inhibition of membrane fusion. T-20 blocks the entry of various HIV-1 strains, even those resistant to inhibitors of reverse transcriptase and/or protease (15, 16). However, T-20-resistant HIV-1 variants, which frequently show mutations in gp41, such as V38A and N43D, have emerged (14, 25, 26, 28, 32). Therefore, novel fusion inhibitors that suppress the replication of T-20-resistant variants are urgently needed.

C34, a C-HR-derived peptide (Fig. 1A), also inhibits fusion in vitro and does so much more efficiently than T-20 (3, 18, 22). Previously, we remodeled C34 by introducing amino acid substitutions that resulted in highly soluble and active derivatives (24). We replaced amino acids at the solvent-accessible site of the helical bundle with glutamate (E) and lysine (K) and maintained those at the interactive site, as these are critical for the interaction with N-HR. In an α-helical heptad repeat, residues separated by three positions (position *i* versus position *i* + 4) are located on the same side of the helix and are closely positioned in space (Fig. 1B). Hence, we introduced consecutive EK motifs separated by three residues (E at positions *i* and *i* + 1 and K at positions *i* + 4 and *i* + 5) of the solvent-accessible site of C34, which resulted in a repeat of the following type: X-EE-XX-KK (where X indicates the original amino acid in HIV-1). A C34 derivative, SC34EK, which has two complete and three incomplete X-EE-XX-KK motifs (Fig. 1), showed enhanced anti-HIV-1 activity compared with that of the parental peptide, C34 (24). A similar result was obtained with T-20EK, the peptide derived by introducing this motif into T-20 (23). Circular dichroism (CD) analysis revealed that both the α-helicity of SC34EK and the thermal stability of the N36-SC34EK complex were enhanced. Interestingly, the antiviral activity of SC35EK, which has five complete X-EE-X X-KK motifs, was comparable to that of SC34EK (24), indicating that five complete X-EE-XX-KK motif repeats are not

* Corresponding author. Mailing address: Laboratory of Virus Control, Institute for Virus Research, Kyoto University, 53 Kawaramachi, Shogoin, Sakyo-ku, Kyoto 606-8507, Japan. Phone and Fax: 81-75-751-3986. E-mail: ekodama@virus.kyoto-u.ac.jp.

▽ Published ahead of print on 29 December 2008.

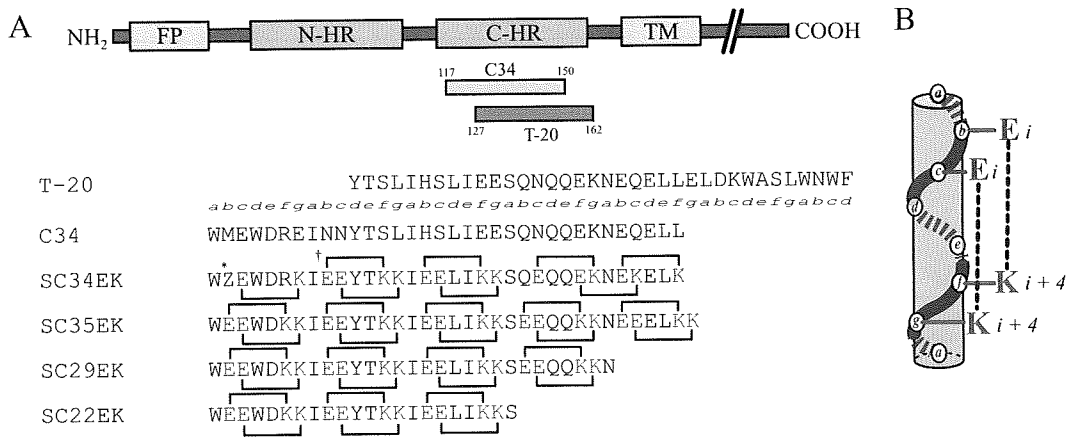

FIG. 1. (A) Schematic diagram of HIV-1 gp41 and sequences of C-HR-derived peptides. FP, fusion peptide; TM, transmembrane domain. The residues at each position in the helical turns are denoted in italics. *Z, an artificial amino acid, norleucine, instead of methionine, to avoid oxidation of the side chain of methionine; †, possible electrostatic interactions indicated by lines and correlating amino acids. (B) One heptad helical turn.

required for strong anti-HIV-1 activity. To address how many complete X-EE-XX-KK motifs are involved in the potent antiviral activity of SC34EK, we synthesized SC29EK and SC22EK (Fig. 1), which contain four and three complete repeats of X-EE-XX-KK, respectively, and evaluated them for their activities against T-20-resistant viruses.

MATERIALS AND METHODS

Cells. HeLa CD4/LTR–β-galactosidase cells obtained from M. Emerman through the AIDS Research and Reference Reagent Program (Germantown, MD) and 293T cells were grown in Dulbecco's modified Eagle medium (DMEM) supplemented with 10% fetal calf serum (FCS), 100 U/ml penicillin G, and 50 μg/ml streptomycin.

Viruses. An HIV-1 infectious clone, pNL4-3 (1), was used for the construction and production of HIV-1 clones. Clones with a certain resistance mutation(s) were introduced by site-directed mutagenesis (29) into the pNL4-3 construct. Although the vast majority of HIV-1 strains have a glycine (G) at position 36 in gp41, the NL4-3 strain used in this study has an aspartic acid (D) residue, which results in impairment of the fusion kinetics of HIV-1 (13, 17). Therefore, in this study, we first constructed a D36G clone, pNL4-3_{D36G}, and used this as a template for the introduction of T-20-resistant mutations, as described previously (21, 31). We constructed three T-20-resistant clones, HIV-$1_{D36G/V38A}$, HIV-$1_{D36G/N43D}$, and HIV-$1_{D36G/N43D/S138A}$ (8), and two C34-resistant clones, HIV-$1_{D36G/N126K}$ and HIV-$1_{\Delta V4/D36G/I37K/N126K/L204I}$ (ΔV4 indicates a five-amino acid [FNSTW] deletion in the V4 region of gp120) (22). Infectious HIV-1 clones were generated by transfection of plasmid clones into 293T cells.

Antiviral agents. Peptide-based fusion inhibitors, including T-20, were synthesized by standard 9-fluorenylmethoxy carbonyl-based solid-phase techniques (24). High-pressure liquid chromatography purification of crude materials on a preparative Cosmosil 5C18 AR-II column with a linear gradient of acetonitrile containing 0.1% trifluoroacetic acid gave the desired peptide samples for biological tests. 2′,3′-Dideoxycytidine (ddC) was purchased from Sigma-Aldrich (St. Louis, MO).

Determination of efficacies of antiviral agents. The efficacies of the antiviral agents were determined by multinuclear activation of galactosidase indicator (MAGI) assays (12, 22). Briefly, 10^4 HeLa CD4/LTR–β-galactosidase cells per well were plated in flat 96-well culture plates. On the following day, the cells were inoculated with the HIV-1 clones (60 MAGI U/well, which gave 60 blue cells after 48 h of incubation) and were cultured in the presence of various concentrations of drugs in fresh medium. After incubation for 48 h after virus inoculation, all of the blue cells that were stained with 5-bromo-4-chloro-3-indolyl-β-D-galactoside in each well were counted. The activities of the test compounds were determined as the concentration that blocked HIV-1 replication by 50% (the 50% effective concentration [EC_{50}]).

Effect of sera on anti-HIV activity. The effect of the FCS concentration on antiviral activity was measured by MAGI assays with FCS at several concentrations (5, 10, 20, and 50%). The effect of serum components on antiviral activity was assessed by MAGI assays. Briefly, T-20 or SC29EK was dissolved in phosphate-buffered saline (PBS), FCS, or serum freshly prepared from HIV-seronegative healthy volunteers at 4 μM; and the mixtures were incubated for 2 h at 37°C. The mixture was diluted to a concentrations of about 1× or 5× the EC_{50} by using a DMEM-based complete medium supplemented with 10% FCS and was subjected to the MAGI assay.

CD analysis. N36- and C-HR-derived peptide complexes were incubated at 37°C for 30 min (final peptide concentration, 10 μM in PBS). The CD spectra were acquired on a spectropolarimeter (model J-710; Jasco Inc., Tokyo, Japan) at 25°C as the average of eight scans. Thermal stability was assessed by monitoring the change in the CD signal at 222 nm as a function of temperature. Thermal unfolding at intervals of 0.5°C was performed after a 15-min equilibration at the desired temperature and an integration time of 1.0 s. The midpoint of the thermal unfolding transition (melting temperature [T_m]) of each complex was determined from the maximum of the first derivative, with respect to the reciprocal of the temperature, of the $[\theta]_{222}$ values.

RESULTS

Antiviral activities of peptides into which EK is introduced. Because W117, W120, and I124, which are crucial for binding to N-HR (2, 3), are located in the N terminus of C34, we deleted the C-terminal region of SC35EK to produce short peptides. SC29EK, which has four complete X-EE-XX-KK motifs, inhibited HIV-1_{NL4-3} infection at a level comparable to that at which SC34EK did (Table 1). As was observed with SC34EK, SC29EK also maintained an inhibitory effect toward T-20-resistant clones. Although SC34EK blocked the replication of C34-resistant clone HIV-$1_{\Delta V4/D36G/I37K/N126K/L204I}$, SC29EK failed to do so. On the other hand, C29, with a 5-amino-acid deletion from the C terminus of C34, exerted drastically reduced antiviral activity. SC22EK, which consisted of three X-EE-XX-KK motifs, also showed much reduced antiviral activity compared with the activities of SC29EK and SC34EK. A native peptide corresponding to SC22EK, C22, exhibited no activity against HIV-1_{NL4-3} at concentrations up to 10 μM (data not shown). Thus, to inhibit the physiological interaction of N-HR and C-HR, a peptide 22 amino acids in length, without modification, may be insufficient. The D36G substitution enhanced the susceptibility of HIV-1 to T-20 (28) but not to C34 or its derivatives (Table 1). These results suggest that four X-EE-XX-KK motifs are required to maintain

TABLE 1. Activities of HIV-1 gp41-derived peptides against T-20-resistant mutants

Virus	EC_{50}[a] (nM)					
	T-20	SC22EK	C29	SC29EK	C34	SC34EK
$HIV\text{-}1_{NL4\text{-}3}$	15 ± 1 (6.3)	217 ± 41 (0.3)	245 ± 42 (4.7)	2.4 ± 0.1 (1.3)	2.3 ± 0.1 (1.0)	1.6 ± 0.2 (0.7)
$HIV\text{-}1_{D36G}$	2.4 ± 0.6	686 ± 94	52 ± 18	1.9 ± 0.0	2.3 ± 0.6	2.4 ± 1.0
$HIV\text{-}1_{D36G/V38A}$	23 ± 8 (9.6)	289 ± 84 (0.4)	504 ± 193 (9.7)	3.0 ± 0.6 (1.6)	4.4 ± 1.4 (1.9)	2.2 ± 0.4 (0.9)
$HIV\text{-}1_{D36G/N43D}$	49 ± 10 (20)	114 ± 36 (0.2)	>1,000 (>19)	4.1 ± 0.6 (2.2)	7.9 ± 0.9 (3.4)	1.6 ± 0.4 (0.7)
$HIV\text{-}1_{D36G/N43D/S138A}$	84 ± 16 (35)	>1,000 (>1.5)	>1,000 (>19)	3.4 ± 0.9 (1.8)	15 ± 2 (6.4)	1.5 ± 0.3 (0.6)
$HIV\text{-}1_{D36G/N126K}$	3.4 ± 0.6 (1.4)	>1,000 (>1.5)	192 ± 22 (3.7)	2.7 ± 0.1 (1.4)	7.0 ± 2.0 (3.0)	12 ± 1 (5.0)
$HIV\text{-}1_{\Delta V4/D36G/I37K/N126K/L204I}$[b]	390 ± 155 (163)	252 ± 71 (0.4)	>1,000 (>19)	50 ± 11 (26)	171 ± 15 (74)	3.0 ± 0.2 (1.3)

[a] Antiviral activity, shown as the EC_{50}, was determined by the MAGI assay. Each EC_{50} represents the mean ± standard deviation obtained from at least three independent experiments. The values in parentheses indicate relative changes (*n*-fold) in the EC_{50} compared with the EC_{50} in the presence of the D36G substitution.
[b] ΔV4 indicates a 5-amino-acid deletion (FNSTW) in the V4 region of gp120.

the inhibitory effect of the peptides on the membrane fusion of HIV-1 strains resistant to T-20, as well as $HIV\text{-}1_{NL4\text{-}3}$.

α-Helicity of the six-helix bundle. To elucidate the mechanism by which SC29EK exerts strong anti-HIV activity, we performed CD analysis of the N36-SC29EK complex. The CD spectrum for the N36-SC29EK complex revealed an α-helix conformation with a characteristic double minimum at 208 nm and 222 nm, similar to the conformations of the N36-C34 and N36-SC35EK complexes. The N36-C29 complex showed an α-helical conformation, while a complex of N36 with C22 showed decreased α-helical spectra (Fig. 2A), in direct correlation to moderately and severely decreased antiviral activities of C29 and C22, respectively. The CD spectra of complexes of N36 peptides containing T-20 resistance-associated mutations with SC29EK, $N36_{V38A}$-SC29EK and $N36_{N43D}$-SC29EK, were almost identical to the CD spectrum of N36 with SC29EK, indicating that SC29EK retains binding affinity for the mutated N36 peptides (Fig. 2B). On the other hand, the mutated N36 peptides and C29 complexes showed little α-helical conformation. These results indicate that introduction of the X-EE-X X-KK motif increases the binding affinity of SC29EK for the mutated N36 peptides.

The thermal stabilities of these complexes were assessed by monitoring the shift in $[\theta]_{222}$ (Fig. 2C). A relatively low T_m (48.5°C) (Fig. 2D) and approximately 80% α-helicity at 37°C (Fig. 2C) were observed with the N36-C29 complex, consistent with its moderate antiviral activity (Table 1). The T_ms of N36- and C-HR-derived peptides into which a X-EE-XX-KK motif was introduced were higher than the T_m of the N36-C34 complex (Fig. 2D), while the T_ms of peptides with the native se-

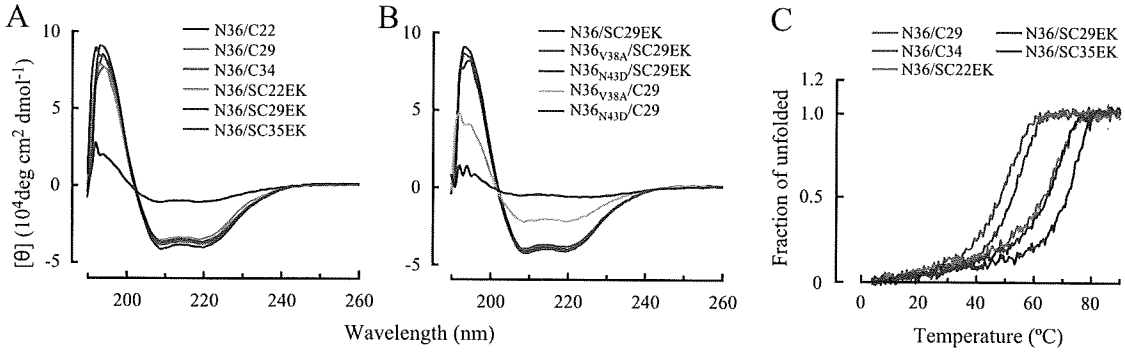

D

peptide		T_m (°C)
N-HR	C-HR	
N36	C29	48.5
N36	C34	52.5
N36	SC22EK	63.5
N36	SC29EK	65
N36	SC35EK	71.5
$N36_{V38A}$	C29	41
$N36_{V38A}$	SC29EK	56
$N36_{N43D}$	C29	NA
$N36_{N43D}$	SC29EK	57

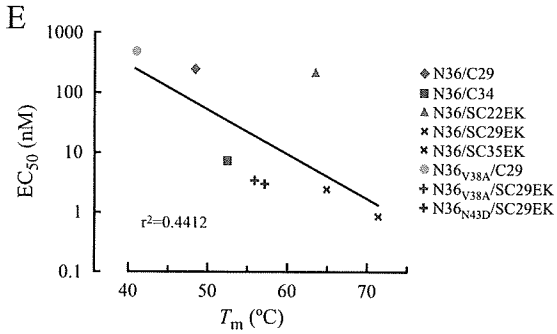

FIG. 2. Analysis of N36 and various C-HR-derived peptides complexes by CD spectroscopy. CD spectra for N36- and C-HR-derived peptide complexes (A) and mutated N36-C29 or SC29EK complexes (B). (C) Temperature-dependent transitions of the dissociation degree of N36 and various C-HR-derived peptide complexes. (D) T_ms of complexes of various N-HR peptides and C-HR peptides. NA, not available. (E) Relation between EC_{50}s of C-HR-derived peptides and T_ms of N36 and various C-HR-derived peptide complexes. The strength of the correlation between EC_{50}s and T_ms is increased (r^2 = 0.8002) when the data for SC22EK are excluded.

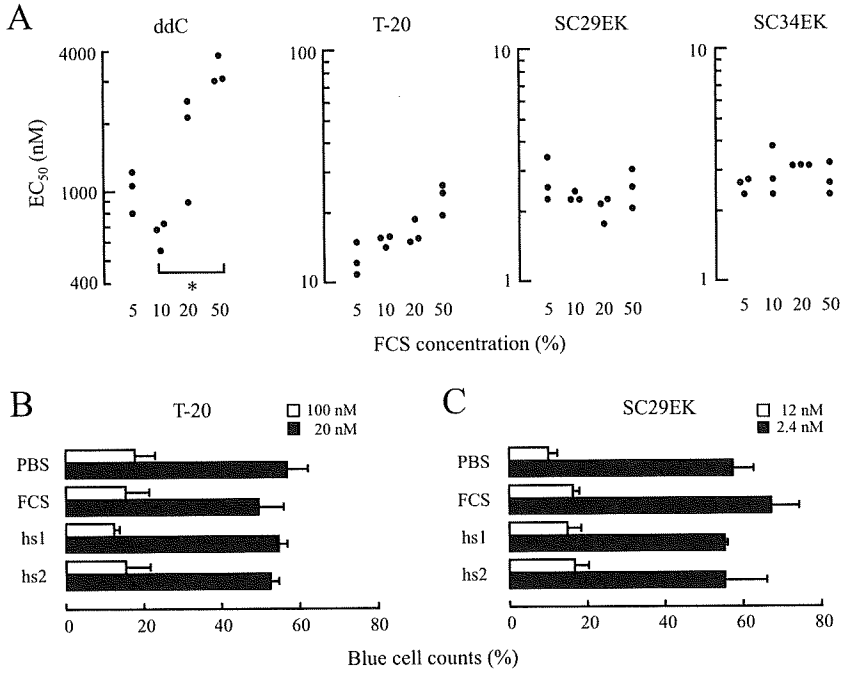

FIG. 3. Effect of serum components on antiviral activity. Antiviral activities in the presence of serum at various concentrations (5, 10, 20, and 50%) were determined by the MAGI assay. (A) Black dots indicate EC_{50}s (nM), each of which was determined three times independently (*, $P = 0.01$ by Student's t test). Antiviral activities of T-20 (B) and SC29EK (C) in human HIV-seronegative sera (hs1 and hs2) were assessed by counting the number of blue cells. Bars indicate the percentages of blue cell counts in PBS, FCS, and human serum compared with the count obtained with no antiviral agents (control, for which the value was 100%). Error bars represent the standard deviation of each mean.

quence but without the introduced motif were lower. The relationships between the EC_{50}s of C-HR-derived peptides and their T_ms are shown in Fig. 2E. The correlation between the EC_{50} and the T_ms was weak ($r^2 = 0.4412$); however, with the exclusion of the data for SC22EK, which showed weak antiviral activity, despite its high T_m, the strength of this correlation was increased ($r^2 = 0.8002$), suggesting that other factors, including solubility and intrapeptide interactions, may be involved in the enhanced antiviral activity of EK-containing peptides.

Effect of serum on antiviral activity. Finally, we assessed the anti-HIV activity of SC29EK in the presence of a high concentration of FCS and in fresh human serum. The activities against HIV-1_{NL4-3} in the presence of various concentrations of FCS (5, 10, 20, and 50%) were determined. A reverse transcriptase inhibitor, ddC, was used as a control. The antiviral activity of ddC was decreased in a concentration-dependent manner (Fig. 3A). In the presence of 50% FCS, the reduction in the EC_{50} of ddC was statistically significant ($P = 0.01$). Similarly, but to a much lesser extent, the EC_{50} of T-20 appeared to be reduced with the FCS concentration in a concentration-dependent manner. Even in the presence of 50% FCS, the mean EC_{50} was comparable to the EC_{50}s in 5% and 10% FCS ($P = 0.082$ and 0.075, respectively). However, the effects of SC29EK and SC34EK were less affected by increased FCS concentrations.

For further evaluation, sera freshly isolated from two HIV-seronegative healthy volunteers were prepared. T-20 and SC29EK incubated for 2 h at 37°C in fresh human serum, FCS, or PBS were diluted with a DMEM-based complete medium supplemented with 10% FCS and were subjected to the MAGI assay. The final FCS concentrations in the various sera that included FCS in these diluted mixtures ranged from 9.75 to 12.2%. Because the antiviral activities of T-20 and SC29EK were not significantly influenced by the FCS concentration (Fig. 3A), it is unlikely that the differences in the FCS concentrations in this experiment had any effect on their antiviral activities. Compared with the inhibitory effects of the PBS-treated peptides, small changes in the inhibitory effects of both T-20 and SC29EK treated with FCS and human sera were observed (Fig. 3B and C). Taken together, these findings suggest that SC29EK stably exerts its strong anti-HIV-1 activity in vivo in the same manner that T-20 does.

DISCUSSION

We show here that SC29EK inhibits the membrane fusion of T-20-resistant HIV-1 strains, suggesting that four X-EE-X X-KK motifs are sufficient to inhibit the fusion of T-20-resistant variants. As revealed by the EC_{50}s and T_ms (Table 1 and Fig. 2), resistance-associated mutations in the N-HR region, such as V38A and N43D, seem to decrease the binding affinity of C-HR-derived peptides for N-HR. Therefore, HIV-1 strains with V38A or N43D show resistance to T-20. However, the anti-HIV-1 activity of SC29EK was less affected by these mutations, because at the physiological temperature for HIV-1 replication, SC29EK showed a stable interaction with N36 peptides containing mutations conferring resistance to T-20. The activity of SC29EK against the C34-resistant clone HIV-$1_{\Delta V4/D36G/I37K/N126K/L204I}$ was decreased, while SC34EK maintained its activity. One of the primary mutations underlying C34 resistance, I37K, is located close to but outside of the

putative binding site of SC29EK. Previously, we reported that an N126K substitution in C-HR enhances the intra-gp41 binding of N-HR and C-HR (22); therefore, we hypothesized that the activity of SC29EK might be decreased by competition with C-HR with the N126K mutation. However, SC29EK also inhibits the entry of HIV-$1_{D36G/N126K}$. Although no structural analysis of the mutated six-helix bundle was performed, it is possible that mutations conferring C34 resistance might induce some structural changes at or adjacent to the SC29EK binding site, because a peptide shortened by a further 7 amino acids, SC22EK, suppressed the entry of the C34-resistant clone.

C34 itself did not have an α-helical spectrum, while SC29EK did (data not shown). SC29EK may achieve its strong antiviral activity by forming an α-helix as a result of E/K substitutions on the solvent-accessible site (Fig. 1). CD analysis shows that HIV-1 builds up resistance to T-20 by introducing certain mutations in N-HR, such as V38A and N43D, which reduce the binding affinity between N-HR and C-HR. SC29EK can efficiently inhibit the fusion of these mutant HIV-1 strains, suggesting that the ability of SC29EK to bind to mutated N-HR and its weak affinity for C-HR are maintained. On the other hand, the D36G, N126K, and S138A mutations increase viral fusion activity (13) by enhancement of the binding affinity of C-HR for N-HR (22, 31). SC29EK effectively suppresses the replication of viruses that have these mutations, such as HIV-1_{D36G}, HIV-$1_{D36G/N43D/S138A}$, and HIV-$1_{D36G/N126K}$. This indicates that the binding capacity of SC29EK is stronger than that of mutated C-HR containing the N126K or the S138A mutation. Therefore, the monomeric α-helical form may inhibit the interactions of N-HR and C-HR with mutations that affect their binding affinity and thus the formation of the six-helix bundle.

Although SC22EK has enhanced α-helicity and a high T_m, it has less antiviral activity than SC29EK. In the interaction between N-HR- and C-HR-derived peptides, while the cavity-forming region (from L54 to Q66) of the C terminus of N-HR (the "pocket") and the cavity-binding region (side chains of W117, W120, and I124) of the N terminus of C-HR (the "knob") play an important role (2, 3, 10), another region of C-HR may also be required. A constrained 14-residue peptide (C14linkmid), which corresponds to the knob region, shows chemical cross-linking and contains amino acid substitutions (27), and it is about 15,000-fold less active than SC29EK, which contains proximal regions in addition to the knob region. These findings also suggest that the knob region of C-HR is important but not sufficient for the formation of a stable complex. Another possible explanation of the weak activity of C14linkmid is that because not only the binding of N-HR and C-HR but also dynamic structural changes are easily anticipated during fusion, it would be difficult to maintain tight binding to the target N-HR due to its rigid constrained form. To maintain the binding of C-HR to N-HR despite such drastic conformational changes during fusion, there may be some unknown interaction, besides the interaction between the pocket and the knob regions, that is necessary for membrane fusion. At present, we cannot conclude whether (i) the length of the peptide itself is crucial, (ii) some other domain has a role, or (iii) a combination of both is important. Further experiments will be needed to clarify the mechanism of inhibition. Such information will be valuable for the generation of effective short peptide inhibitors or small molecules. To generate effective small-molecule inhibitors, if the second possibility is correct, a combination of two agents, one of which interacts with the pocket and the other of which interacts with an unidentified domain, should provide enhanced efficacy. To date, only a limited number of small-molecule compounds that inhibit the six-helix bundle formation with marginal activities have been reported (5, 9, 11), although among the peptide-based inhibitors, several effective peptides have been developed, including T1249 (7), SC34EK (24), T2635 (6), and T-20EK (23).

The T_m of the N36-SC29EK complex was higher than that of the N36-C29 complex, suggesting that EK substitutions reinforced the affinity of binding to N-HR through enhanced α-helicity. It has been considered that the enhanced α-helical structure is maintained by intrahelical salt bridges formed by the introduction of EK substitutions (19). We recently revealed that an electrostatic interaction formed by the EK alignment is involved in enhanced α-helicity (22a), indicating that the strong α-helical stability of SC29EK is probably provided by a mechanism identical to that for SC34EK. Similar peptides with substitutions of glutamate and arginine provided to increase α-helicity have been reported (6). These peptides also increase the stability of the helix and have activity against T-20-resistant HIV-1. Moreover, these peptides were relatively stable in an in vivo model. It is possible that enhanced binding affinity confers nonspecific binding to other α-helical regions of cellular proteins, for example, human serum albumin, which contains 31 α-helical regions (20). However, this effect will be minimal, because the antiviral activity of SC29EK was highly stable in the presence of higher concentrations of FCS and was less affected by human serum.

In this study, we demonstrated that a 29-amino-acid short peptide, SC29EK, suppresses the replication of T-20-resistant variants. SC29EK maintained its activity in the presence of high concentrations of sera, indicating that SC29EK is a candidate short peptide fusion inhibitor.

ACKNOWLEDGMENTS

This work was supported in part by a grant for Research for Health Sciences Focusing on Drug Innovation from the Japan Health Sciences Foundation (E.K., S.O., N.F., M.M.) and a grant for the Promotion of AIDS Research from the Ministry of Health and Welfare of Japan (M.M.). T.N., K.I., and H.N. are supported by the 21st Century COE Program of the Ministry of Education, Culture, Sports, Science, and Technology. S.G.S. was supported by the National Institutes of Health (grants R01AI076119 and 1R21AI079801).

REFERENCES

1. **Adachi, A., H. E. Gendelman, S. Koenig, T. Folks, R. Willey, A. Rabson, and M. A. Martin.** 1986. Production of acquired immunodeficiency syndrome-associated retrovirus in human and nonhuman cells transfected with an infectious molecular clone. J. Virol. **59**:284–291.
2. **Chan, D. C., C. T. Chutkowski, and P. S. Kim.** 1998. Evidence that a prominent cavity in the coiled coil of HIV type 1 gp41 is an attractive drug target. Proc. Natl. Acad. Sci. USA **95**:15613–15617.
3. **Chan, D. C., D. Fass, J. M. Berger, and P. S. Kim.** 1997. Core structure of gp41 from the HIV envelope glycoprotein. Cell **89**:263–273.
4. **Chan, D. C., and P. S. Kim.** 1998. HIV entry and its inhibition. Cell **93**:681–684.
5. **Cianci, C., D. R. Langley, D. D. Dischino, Y. Sun, K. L. Yu, A. Stanley, J. Roach, Z. Li, R. Dalterio, R. Colonno, N. A. Meanwell, and M. Krystal.** 2004. Targeting a binding pocket within the trimer-of-hairpins: small-molecule inhibition of viral fusion. Proc. Natl. Acad. Sci. USA **101**:15046–15051.
6. **Dwyer, J. J., K. L. Wilson, D. K. Davison, S. A. Freel, J. E. Seedorff, S. A. Wring, N. A. Tvermoes, T. J. Matthews, M. L. Greenberg, and M. K. Delmedico.** 2007. Design of helical, oligomeric HIV-1 fusion inhibitor peptides

with potent activity against enfuvirtide-resistant virus. Proc. Natl. Acad. Sci. USA **104:**12772–12777.

7. **Eron, J. J., R. M. Gulick, J. A. Bartlett, T. Merigan, R. Arduino, J. M. Kilby, B. Yangco, A. Diers, C. Drobnes, R. DeMasi, M. Greenberg, T. Melby, C. Raskino, P. Rusnak, Y. Zhang, R. Spence, and G. D. Miralles.** 2004. Short-term safety and antiretroviral activity of T-1249, a second-generation fusion inhibitor of HIV. J. Infect. Dis. **189:**1075–1083.
8. **Fikkert, V., P. Cherepanov, K. Van Laethem, A. Hantson, B. Van Remoortel, C. Pannecouque, E. De Clercq, Z. Debyser, A. M. Vandamme, and M. Witvrouw.** 2002. *env* chimeric virus technology for evaluating human immunodeficiency virus susceptibility to entry inhibitors. Antimicrob. Agents Chemother. **46:**3954–3962.
9. **Frey, G., S. Rits-Volloch, X. Q. Zhang, R. T. Schooley, B. Chen, and S. C. Harrison.** 2006. Small molecules that bind the inner core of gp41 and inhibit HIV envelope-mediated fusion. Proc. Natl. Acad. Sci. USA **103:** 13938–13943.
10. **Ji, H., W. Shu, F. T. Burling, S. Jiang, and M. Lu.** 1999. Inhibition of human immunodeficiency virus type 1 infectivity by the gp41 core: role of a conserved hydrophobic cavity in membrane fusion. J. Virol. **73:**8578–8586.
11. **Jiang, S., H. Lu, S. Liu, Q. Zhao, Y. He, and A. K. Debnath.** 2004. N-substituted pyrrole derivatives as novel human immunodeficiency virus type 1 entry inhibitors that interfere with the gp41 six-helix bundle formation and block virus fusion. Antimicrob. Agents Chemother. **48:**4349–4359.
12. **Kimpton, J., and M. Emerman.** 1992. Detection of replication-competent and pseudotyped human immunodeficiency virus with a sensitive cell line on the basis of activation of an integrated beta-galactosidase gene. J. Virol. **66:**2232–2239.
13. **Kinomoto, M., M. Yokoyama, H. Sato, A. Kojima, T. Kurata, K. Ikuta, T. Sata, and K. Tokunaga.** 2005. Amino acid 36 in the human immunodeficiency virus type 1 gp41 ectodomain controls fusogenic activity: implications for the molecular mechanism of viral escape from a fusion inhibitor. J. Virol. **79:**5996–6004.
14. **Labrosse, B., L. Morand-Joubert, A. Goubard, S. Rochas, J. L. Labernardiere, J. Pacanowski, J. L. Meynard, A. J. Hance, F. Clavel, and F. Mammano.** 2006. Role of the envelope genetic context in the development of enfuvirtide resistance in human immunodeficiency virus type 1-infected patients. J. Virol. **80:**8807–8819.
15. **Lalezari, J. P., K. Henry, M. O'Hearn, J. S. Montaner, P. J. Piliero, B. Trottier, S. Walmsley, C. Cohen, D. R. Kuritzkes, J. J. Eron, Jr., J. Chung, R. DeMasi, L. Donatacci, C. Drobnes, J. Delehanty, and M. Salgo.** 2003. Enfuvirtide, an HIV-1 fusion inhibitor, for drug-resistant HIV infection in North and South America. N. Engl. J. Med. **348:**2175–2185.
16. **Lazzarin, A., B. Clotet, D. Cooper, J. Reynes, K. Arasteh, M. Nelson, C. Katlama, H. J. Stellbrink, J. F. Delfraissy, J. Lange, L. Huson, R. DeMasi, C. Wat, J. Delehanty, C. Drobnes, and M. Salgo.** 2003. Efficacy of enfuvirtide in patients infected with drug-resistant HIV-1 in Europe and Australia. N. Engl. J. Med. **348:**2186–2195.
17. **Lu, J., P. Sista, F. Giguel, M. Greenberg, and D. R. Kuritzkes.** 2004. Relative replicative fitness of human immunodeficiency virus type 1 mutants resistant to enfuvirtide (T-20). J. Virol. **78:**4628–4637.
18. **Lu, M., and P. S. Kim.** 1997. A trimeric structural subdomain of the HIV-1 transmembrane glycoprotein. J. Biomol. Struct. Dyn. **15:**465–471.
19. **Marqusee, S., and R. L. Baldwin.** 1987. Helix stabilization by Glu− . . . Lys+ salt bridges in short peptides of de novo design. Proc. Natl. Acad. Sci. USA **84:**8898–8902.
20. **Matsuo, K., R. Yonehara, and K. Gekko.** 2004. Secondary-structure analysis of proteins by vacuum-ultraviolet circular dichroism spectroscopy. J. Biochem. **135:**405–411.
21. **Mink, M., S. M. Mosier, S. Janumpalli, D. Davison, L. Jin, T. Melby, P. Sista, J. Erickson, D. Lambert, S. A. Stanfield-Oakley, M. Salgo, N. Cammack, T. Matthews, and M. L. Greenberg.** 2005. Impact of human immunodeficiency virus type 1 gp41 amino acid substitutions selected during enfuvirtide treatment on gp41 binding and antiviral potency of enfuvirtide in vitro. J. Virol. **79:**12447–12454.
22. **Nameki, D., E. Kodama, M. Ikeuchi, N. Mabuchi, A. Otaka, H. Tamamura, M. Ohno, N. Fujii, and M. Matsuoka.** 2005. Mutations conferring resistance to human immunodeficiency virus type 1 fusion inhibitors are restricted by gp41 and Rev-responsive element functions. J. Virol. **79:**764–770.

22a. **Nishikawa, H., S. Nakamura, E. Kodama, S. Ito, K. Kajiwara, K. Izumi, Y. Sakagami, S. Oishi, T. Ohkubo, Y. Kobayashi, A. Otaka, N. Fujii, and M. Matsuoka.** Electrostatically constrained alpha-helical peptide inhibits replication of HIV-1 resistant to enfuvirtide. Int. J. Biochem. Cell Biol., in press.

23. **Oishi, S., S. Ito, H. Nishikawa, K. Watanabe, M. Tanaka, H. Ohno, K. Izumi, Y. Sakagami, E. Kodama, M. Matsuoka, and N. Fujii.** 2008. Design of a novel HIV-1 fusion inhibitor that displays a minimal interface for binding affinity. J. Med. Chem. **51:**388–391.
24. **Otaka, A., M. Nakamura, D. Nameki, E. Kodama, S. Uchiyama, S. Nakamura, H. Nakano, H. Tamamura, Y. Kobayashi, M. Matsuoka, and N. Fujii.** 2002. Remodeling of gp41-C34 peptide leads to highly effective inhibitors of the fusion of HIV-1 with target cells. Angew. Chem. Int. Ed. Engl. **41:**2937–2940.
25. **Poveda, E., B. Rodes, C. Toro, L. Martin-Carbonero, J. Gonzalez-Lahoz, and V. Soriano.** 2002. Evolution of the gp41 *env* region in HIV-infected patients receiving T-20, a fusion inhibitor. AIDS **16:**1959–1961.
26. **Rimsky, L. T., D. C. Shugars, and T. J. Matthews.** 1998. Determinants of human immunodeficiency virus type 1 resistance to gp41-derived inhibitory peptides. J. Virol. **72:**986–993.
27. **Sia, S. K., P. A. Carr, A. G. Cochran, V. N. Malashkevich, and P. S. Kim.** 2002. Short constrained peptides that inhibit HIV-1 entry. Proc. Natl. Acad. Sci. USA **99:**14664–14669.
28. **Wei, X., J. M. Decker, H. Liu, Z. Zhang, R. B. Arani, J. M. Kilby, M. S. Saag, X. Wu, G. M. Shaw, and J. C. Kappes.** 2002. Emergence of resistant human immunodeficiency virus type 1 in patients receiving fusion inhibitor (T-20) monotherapy. Antimicrob. Agents Chemother. **46:**1896–1905.
29. **Weiner, M. P., G. L. Costa, W. Schoettlin, J. Cline, E. Mathur, and J. C. Bauer.** 1994. Site-directed mutagenesis of double-stranded DNA by the polymerase chain reaction. Gene **151:**119–123.
30. **Wild, C., T. Greenwell, and T. Matthews.** 1993. A synthetic peptide from HIV-1 gp41 is a potent inhibitor of virus-mediated cell-cell fusion. AIDS Res. Hum. Retrovir. **9:**1051–1053.
31. **Xu, L., A. Pozniak, A. Wildfire, S. A. Stanfield-Oakley, S. M. Mosier, D. Ratcliffe, J. Workman, A. Joall, R. Myers, E. Smit, P. A. Cane, M. L. Greenberg, and D. Pillay.** 2005. Emergence and evolution of enfuvirtide resistance following long-term therapy involves heptad repeat 2 mutations within gp41. Antimicrob. Agents Chemother. **49:**1113–1119.
32. **Zollner, B., H. H. Feucht, M. Schroter, P. Schafer, A. Plettenberg, A. Stoehr, and R. Laufs.** 2001. Primary genotypic resistance of HIV-1 to the fusion inhibitor T-20 in long-term infected patients. AIDS **15:**935–936.

Antiviral Research 82 (2009) 67–72

Contents lists available at ScienceDirect

Antiviral Research

journal homepage: www.elsevier.com/locate/antiviral

Synonymous mutations in stem-loop III of Rev responsive elements enhance HIV-1 replication impaired by primary mutations for resistance to enfuvirtide

Mariko Ueno[a,b,1], Eiichi N. Kodama[a,*], Kazuya Shimura[a], Yasuteru Sakurai[a,b], Keiko Kajiwara[a,b], Yasuko Sakagami[a], Shinya Oishi[c], Nobutaka Fujii[c], Masao Matsuoka[a]

[a] Laboratory of Virus Control, Institute for Virus Research, Kyoto University, 53 Kawaramachi, Shogoin, Sakyo-ku, Kyoto 606-8507, Japan
[b] Graduate School of Biostudies, Kyoto University, Kyoto, Japan
[c] Graduate School of Pharmaceutical Science, Kyoto University, Kyoto, Japan

ARTICLE INFO

Article history:
Received 9 May 2008
Received in revised form 16 December 2008
Accepted 3 February 2009

Keywords:
Fusion
gp41
Rev responsive element
Secondary mutation
HIV-1
Replication

ABSTRACT

Primary mutations in HIV-1 that are directly involved in the resistance to enfuvirtide have been well documented. However, secondary mutations that are associated with primary mutations and contribute little to the resistance still remain to be elucidated. This study reveals that synonymous mutations at gp41 Q41 (CAG to CAA) or L44 (UUG to CUG) act as secondary mutations. Complementary mutations in the nucleotide level are located in the Rev responsive element (RRE) of the HIV-1 RNA-genome and maintain the replication kinetics of HIV-1 through increasing the structural stability of stem-loop III in the RRE. Therefore, synonymous mutations in the gp41/RRE sequence improve the viral replication impaired by the primary mutations and play a key role as secondary (complementary) mutations.

1. Introduction

Enfuvirtide (T-20), an HIV-1 fusion inhibitor which has been approved for the treatment of HIV-1 infected patients, successfully suppresses the replication of HIV-1 even in strains resistant to various reverse transcriptase and protease inhibitors (Fung and Guo, 2004; Lalezari et al., 2003; Lazzarin et al., 2003; Manfredi and Sabbatani, 2006). However, HIV-1 variants resistant to T-20 have emerged after prolonged T-20 therapy (Lu et al., 2006; Marcelin et al., 2004; Sista et al., 2004; Wei et al., 2002). The majority of resistant variants develop primary mutations to T-20, including V38A and N43D, in the consensus sequence, GIVQQQNNLL (DIVQQQNNLL for NL4-3) motif of the gp41 within amino acid positions 36–45 (Cabrera et al., 2006; Fikkert et al., 2002; Lu et al., 2006; Marcelin et al., 2004; Menzo et al., 2004; Mink et al., 2005; Poveda et al., 2002; Sista et al., 2004; Su et al., 2006; Wei et al., 2002). Few studies have so far addressed secondary mutations for resistance to T-20.

Primary and secondary mutations were recently well-defined for C34, a peptide derived from the gp41 carboxyl terminus heptad repeat (C-HR) in vitro (Nameki et al., 2005). A30V and D36G in the gp41 act as secondary mutations which enhance the replication kinetics impaired by primary mutations. Interestingly, these mutations are complementarily located in stem-loop IIA and C (Fig. 1) of the Rev responsive element (RRE) which is an essential RNA structure for transporting non- and singly spliced viral RNA to the cytoplasm from the nucleus (Olsen et al., 1990; Zapp and Green, 1989). Most recently, T18A and V38A complementarily located in the stem IIA of the RRE has been detected in clinical isolates treated with T-20 (Svicher et al., 2008). Co-presence of T18A and V38A is associated with high level of viral load. These data support our recent in vitro results that these secondary mutations in stem II maintain HIV-1 replication through substitutions at the nucleotide as well as the amino acid level (Nameki et al., 2005). This study analyzed the nucleotide sequences of T-20 resistant variants deposited in the GenBank (http://www.ncbi.nlm.nih.gov/Genbank) and revealed that synonymous mutations in stem-loop III of the RRE maintain HIV-1 replication impaired by N43D, one of primary mutations for T-20 resistance.

2. Materials and methods

2.1. Antiviral agents and cells

T-20 was synthesized as described previously (Otaka et al., 2002). 2′,3′-Dideoxycytidine (ddC) was purchased from Sigma (St.

* Corresponding author. Tel.: +81 75 751 3986; fax: +81 75 751 3986.
E-mail address: ekodama@virus.kyoto-u.ac.jp (E.N. Kodama).
[1] The author has been moved to Kureha Corporation, Tokyo, Japan.

0166-3542/$ – see front matter © 2009 Elsevier B.V. All rights reserved.
doi:10.1016/j.antiviral.2009.02.002

(A)

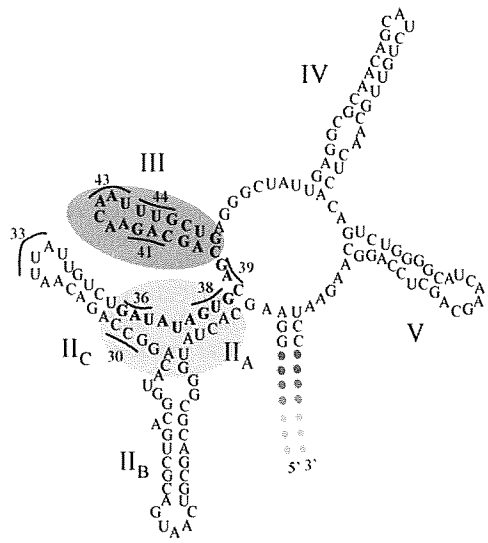

(B)

Mutations: Amino acid	Mutations: Nucleotide	Secondary structure of stem loop III	ΔG (kcal/mol)
None (WT: NL4-3)	None		-6.5
Q39Q	CAG → CA**A**	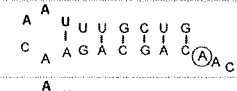	-6.8
Q41Q	CAG → CA**A**	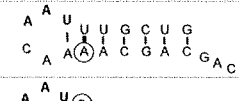	-6.4
L44L	UUG → **C**UG		-9.1
L44L	UUG → **UU**A		0.1
N43D	AAU → **G**AU	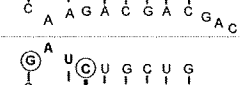	-6.5
N43D L44L	AAU → **G**AU UUG → **C**UG		-9.0
Q39Q N43D	CAG → CA**A** AAU → **G**AU		-6.8
Q41Q N43D	CAG → CA**A** AAU → **G**AU	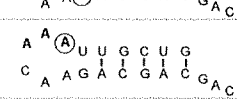	-6.4
N43K	AAU → AA**A**	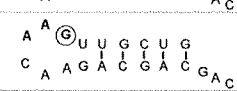	-4.9
N43K	AAU → AA**G**	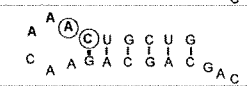	-5.4
N43K L44L	AAU → AA**A** UUG → **C**UG	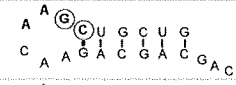	-7.7
N43K L44L	AAU → AA**G** UUG → **C**UG	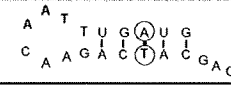	-7.9
Q40H L45M	CAG → CA**T** CUG → **A**UG	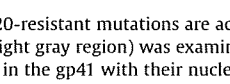	-4.5

(C)

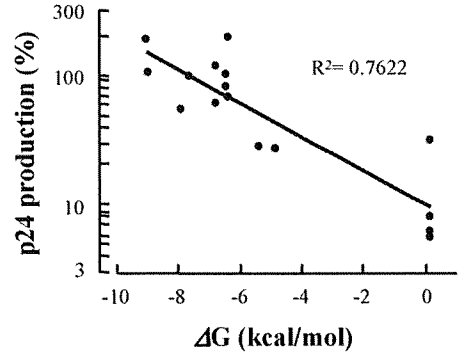

Fig. 1. (A) Secondary structure of RRE depicted based on references (Olsen et al., 1990; Zapp and Green, 1989). T-20-resistant mutations are accumulated between amino acid position from 36 to 45 of gp41 and nucleotides coding for these amino acids, are given in bold. Stem-loop II (light gray region) was examined as described previously (Nameki et al., 2005) and stem-loop III (dark gray region) was analyzed in this study. (B) Amino acid substitutions in the gp41 with their nucleotide changes and putative secondary structures and their stabilities of stem-loop III are shown. Nucleotide substitutions are indicated in bold and circle. Newly generated nucleotide pairs are indicated by the bold line. The stability of stem-loop III defined by ΔG value was calculated using the MFold program version 3.2 (Mathews et al., 1999; Zuker, 2003). (C) Correlation of the amounts of p24 production and stability of stem-loop III (ΔG value) is shown. Plots of Q41H and L45M were included (see text) but that of V38A was excluded since V38A is located in stem IIA. Since replication of N43D containing clones were extremely low, p24 productions obtained from D36G combined N43D or K containing clones, were used. When excluding data of D36G combined with N43D or N43K and including that of N43K without D36G, correlation coefficient (R^2) was 0.72.

Louis, MO). HeLa-CD4-LTR-β-gal cells were used for the drug susceptibility assay (MAGI assay) as described (Nameki et al., 2005). MT-2 and 293T cells were grown in RPMI1640- and Dulbecco's modified Eagle's medium (DMEM)-based culture medium, respectively.

2.2. Generation of recombinant viruses

An HIV-1 infectious clone, pNL4-3, which was kindly provided by Dr. H. Sakai, Institute for Virus Research, Kyoto University (Kyoto, Japan), was used for the construction and the production of HIV-1 variants. To generate major T-20-resistent molecular clones, desired mutations were introduced into the Nhe I-BamH I region (1221 bp) of pSLgp41WT, which encoded nucleotides 7250–8470 of pNL4-3, by site-directed mutagenesis as described (Nameki et al., 2005). The Nhe I-BamH I fragments were then inserted into pNL4-3, generating various molecular clones with the desired mutations. Viruses were recovered from the supernatant of the transfected 293T cells and stored at −80 °C until use. A wild type HIV-1, HIV-1WT, was generated by transfection of pNL4-3 into 293T cells.

2.3. Determination of titer and drug susceptibility of HIV-1

The titer and peptide-sensitivity of infectious clones was determined by the MAGI assay with some modifications (Kimpton and Emerman, 1992; Kodama et al., 2001; Maeda et al., 1998). Briefly, the target cells (HeLa-CD4-LTR-β-gal; 10^4 cells/well) were plated in 96-well flat microtiter culture plates. On the following day, the cells were inoculated with the supernatant of 293T cells transfected with HIV-1 clones and the titrated HIV-1 clones in the presence of various concentrations of drugs in fresh medium, for determination

of titer and drug susceptibility of HIV-1, respectively. Forty-eight hours after the viral exposure, all the blue cells stained with X-Gal were counted in each well. Viral titer was determined with the MAGI assay as blue cell forming units (BFUs). The activity of test compounds was determined as the concentration that blocked HIV-1 replication by 50% (EC_{50}).

2.4. Viral replication kinetics assay

MT-2 cells (10^5 cells) were infected with each virus preparation (500 BFUs) derived from molecular-constructed clone for 4 h. The infected cells were washed and cultured in a volume of 3 ml. The culture supernatants were harvested on day 4 after infection during the linear replication phase and p24 antigen production was determined (Hachiya et al., 2008). For competitive HIV-1 replication assays (CHRA), the two titrated infectious clones were mixed and added to MT-2 cells as described previously (Nameki et al., 2005). To ensure that the two infectious clones being compared were of approximately equal infectivity, a fixed amount (500 BFUs) of one infectious clone was mixed with three different amounts (250, 500 and 1000 BFUs) of the other infectious clone. On day 1, one-third of the infected MT-2 cells were harvested, and subjected to DNA extraction. The purified DNA was used for nested PCR and then direct sequencing. Every 4–5 days, the viral population change was also determined, and the cell-free supernatant of the virus coculture (1 ml) was transmitted to new uninfected MT-2 cells. The cells harvested at the end of each passage were subjected to direct sequencing, and the viral population change was determined.

2.5. GenBank accession numbers

All sequences of clinical isolates referred in this study are available under GenBank accession nos. AF500084 to AF500093, AJ964904 to AJ964940, AY185366 to AY185492, AY436381 to AY436401, AY523979 to AY523991, AY750998 to AY751078, AY768582 to AY768660, and AY785131 to AY785135.

3. Results

3.1. T-20 susceptibility of HIV-1 clones

V38A, N43D, and a combination of Q40H and L45M conferred strong resistance to T-20 (more than 48-fold) while the Q40H, N43K, and L45M substitutions conferred moderate resistance (5.4–13-fold) in comparison to NL4-3 (wild type, WT) (Table 1). These results are consistent with those of a previous report (Labrosse et al., 2006; Lu et al., 2004; Menzo et al., 2004; Pérez-Alvarez et al., 2006; Wei et al., 2002) and demonstrate that these substitutions act as a primary mutation for T-20 resistance. All synonymous mutations at 39, 41, and 44 conferred little T-20 resistance by themselves and even in combination with other substitutions, including N43D and N43K (Table 1). Since Q39, located adjacent to stem-loop III, has no complementary partner, Q39 was used for further experiments as a control for synonymous mutations. Therefore, the gp41 amino acid sequence solely confers T-20 resistance, while the RNA sequence or the structure itself may not markedly contribute to T-20 resistance.

Although the D36G substitution located in the stem-loop II is observed in the vast majority of HIV-1 strains, only NL4-3 strain contains D36 at this position. The introduction of D36G into NL4-3 based T-20 resistant clones enhanced T-20 susceptibility by approximately 10-fold (Table 1). The D36G partially or completely restored T-20 susceptibility attenuated by N43D or K in NL4-3 viruses, respectively. Therefore, D36 may actually enhance T-20 resistance caused by N43D or N43K in the vast majority of the HIV-1 strains. In fact, D36 is frequently detected in T-20 experienced patients and is associated with T-20 resistance (Cabrera et al., 2006). However, N43K containing variants with D36G background seem to be insufficient for resistance to T-20 (only 4-fold resistance), which is consistent with low frequency of emergence of N43K containing variants in T-20-experienced patients (Lu et al., 2006; Morozov et al., 2007; Si-Mohamed et al., 2007).

3.2. Replication kinetics

In D36 background (pNL4-3 derived virus), replication of HIV-1 with primary mutation(s) was much attenuated (Table 1). It is well consistent with rare frequency of simultaneous introduction of V38A and/or N43D with D36 in vivo (Cabrera et al., 2006). Synonymous substitutions at amino acids, Q41 and L44 were frequently observed in T-20-resistant clinical isolates with N43 substitutions deposited in the GenBank, suggesting that these synonymous mutations may work as secondary mutations. To prove this hypothesis, N43D mutants were generated with synonymous mutations, L44L-CUG: UUG → CUG, Q39Q-CAA: CAG → CAA and Q41Q-CAA: CAG → CAA, designated as HIV-$1_{N43D/L44L-CUG}$, HIV-$1_{Q39Q-CAA/N43D}$ and HIV-$1_{Q41Q-CAA/N43D}$, respectively, and their replication kinetics were determined. The p24 production of all of the mutants remained less than 2% in comparison to that of HIV-1WT (Table 1). Replication kinetics were compared based on CHRA, demonstrating that combination of synonymous and complementary mutations, Q41Q-CAA and L44L-CUG restored replication kinetics impaired by N43D, while that of a simple synonymous mutation (not complementary), Q39Q-CAA, did not (Table 2). However, the D43N (GAU → AAU) substitution, which reverts to WT sequence, was detected in the virus population as early as on day 10 during the CHRA, when HIV-1N43D was used (Fig. 2). N43D (GAU) is the putative target site of apobec3F or 3G deamination that is involved in innate immunity to HIV-1 infection (Bishop et al., 2004; Harris et al., 2003; Liddament et al., 2004; Mangeat et al., 2003; Wiegand et al., 2004; Zhang et al., 2003). The MT-2 cells used in this study express both apobec 3G and 3F as confirmed by reverse transcription 165 coupled PCR (data not shown). Therefore, N43D might be reverted to N43 (identical sequence of HIV-1WT) by the deaminases, thus resulting in the appearance of NL4-3 strains.

Since D36G increases the level of replication by controlling the fusogenic activity (Kinomoto et al., 2005) and stability of RRE structure (Nameki et al., 2005), the generated N43D mutants were combined with D36G (HIV-$1_{D36G/N43D}$, HIV-$1_{D36G/N43D/L44L-CUG}$, HIV-$1_{D36G/Q39Q-CAA/N43D}$ and HIV-$1_{D36G/Q41Q-CAA/N43D}$). These recombinant viruses showed comparable replication kinetics with HIV-1WT or HIV-1_{D36G} (Table 1) and revealed an identical order of replication observed in the N43D containing HIV-1s by the CHRA (Table 2). It is likely that N43D mainly impaired replication kinetics through altered fusion kinetics, since reduced replication kinetics by N43D can be partially restored by introduction of S138A (Cabrera et al., 2006; Marcial et al., 2006; Mink et al., 2005; Xu et al., 2005) and the ΔG value is identical to that of WT (Fig. 1B). It is also possible that nucleotide sequence of N43D-GAT may influence Rev binding to stem III.

In N43K mutants, the synonymous mutation, L44L-CTG, also enhanced the replication kinetics (Table 2). The L44L-CTG enhancement was greater in N43K-AAA mutant. Taken together, synonymous and complementary mutations restore HIV-1 replication impaired by introduced primary mutations, suggesting that these mutations act as secondary mutations.

3.3. Stability of stem-loop III

The structural stability of stem-loop III for N43K with codons AAA or AAG, were both comparable (Fig. 1) when calculated using

Table 1
Drug susceptibility[a] and viral replication[b] of HIV-1 clones with primary mutations or synonymous mutations.

Mutation(s)	EC_{50} [c] (μM)		p24(%)
	ddC	T-20	
WT[d]	0.51 ± 0.089	0.021 ± 0.0093	100
D36G	0.66 ± 0.22 (1.3)[e]	0.0026 ± 0.0012 (0.1)	95 ± 15
Primary mutations			
V38A	0.65 ± 0.12 (1.3)	>1.0 (>48)	3.3 ± 1.7
Q40H	0.47 ± 0.11 (0.9)	0.21 ± 0.087 (10)	31 ± 11
N43D	0.48 ± 0.13 (0.9)	>1.0 (>48)	<2
$N43K_{AAA}$	0.22 ± 0.005 (0.4)	0.28 ± 0.024 (13)	21 ± 11
$N43K_{AAG}$	0.32 ± 0.009 (0.6)	0.11 ± 0.019 (5.4)	30 ± 16
L45M	0.68 ± 0.12 (1.3)	0.27 ± 0.11 (13)	5.4 ± 0.8
Q40H/L45M	0.37 ± 0.2 (0.7)	>1.0 (>48)	7.7 ± 3.7
Synonymous mutations			
$Q_{CAG}39Q_{CAA}$	0.62 ± 0.077 (1.2)	0.015 ± 0.006 (0.7)	115 ± 16
$Q_{CAG}41Q_{CAA}$	0.58 ± 0.13 (1.1)	0.054 ± 0.011 (2.6)	192 ± 53
$L_{UUG}44L_{CUG}$	0.62 ± 0.089 (1.2)	0.030 ± 0.018 (1.5)	191 ± 34
$L_{UUG}44L_{UUA}$	0.64 ± 0.18 (1.3)	0.014 ± 0.0026 (0.7)	5.9 ± 1.7
N43D series			
N43D[f]	0.48 ± 0.13 (0.9)	>1.0 (>48)	<2[g]
$N43D/L44L_{CUG}$	0.35 ± 0.050 (0.7)	>1.0 (>48)	<2
$Q39Q_{CAA}/N43D$	0.34 ± 0.17 (0.7)	>1.0 (>48)	<2
$Q41Q_{CAA}/N43D$	0.62 ± 0.097 (1.2)	>1.0 (>48)	<2
D36G/N43D	0.56 ± 0.18 (1.1)	0.13 ± 0.056 (6.1)	81 ± 10
$D36G/N43D/L44L_{CUG}$	0.63 ± 0.19 (1.2)	0.10 ± 0.045 (4.9)	103 ± 34
$D36G/Q39Q_{CAA}/N43D$	0.76 ± 0.12 (1.5)	0.14 ± 0.057 (6.8)	59 ± 23
$D36G/Q41Q_{CAA}/N43D$	0.74 ± 0.14 (1.5)	0.14 ± 0.066 (6.8)	67 ± 16
N43K series			
$N43K_{AAA}$ [f]	0.22 ± 0.005 (0.4)	0.28 ± 0.024 (13)	21 ± 11
$N43K_{AAG}$ [f]	0.32 ± 0.009 (0.6)	0.28 ± 0.077 (13)	30 ± 16
$N43K_{AAA}/L44L_{CUG}$	0.64 ± 0.087 (1.3)	0.22 ± 0.082 (11)	76 ± 18
$N43K_{AAG}/L44L_{CUG}$	0.59 ± 0.10 (1.2)	0.20 ± 0.067 (10)	37 ± 15
$D36G/N43K_{AAA}$	0.61 ± 0.086 (1.2)	0.0069 ± 0.0004 (0.3)	26 ± 18
$D36G/N43K_{AAG}$	0.60 ± 0.078 (1.2)	0.0087 ± 0.0008 (0.4)	27 ± 12
$D36G/N43K_{AAA}/L44_{CUG}$	0.28 ± 0.14 (0.6)	0.0057 ± 0.0016 (0.3)	96 ± 19
$D36G/N43K_{AAG}/L44L_{CUG}$	0.69 ± 0.14 (1.4)	0.0069 ± 0.0003 (0.3)	53 ± 8.1

[a] Antiviral activity was determined by the MAGI assay. The data shown are mean values and standard deviations obtained from the results of at least three independent experiments.

[b] Viral replication was determined by p24 ELISA. The data shown are mean values and standard deviations obtained from the results of at least three independent experiments. Absolute p24 value for $HIV\text{-}1_{WT}$ was 1.8 ± 0.2 ng/ml.

[c] 50% effective concentration was determined with the MAGI assay (Nameki et al., 2005).

[d] $HIV\text{-}1_{NL4\text{-}3}$ was used as a wild type virus.

[e] Fold change in EC_{50} of the gp41 recombinant molecular clone compared with that of $HIV\text{-}1_{WT}$.

[f] Also described in the *primary mutations* section of Table 1.

[g] Only insufficient replication of $HIV\text{-}1_{N43D}$ in MT-2 cells was observed. However, we could determine initial titer of the $HIV\text{-}1_{N43D}$ obtained from freshly transfected 293T cells in the MAGI cells, since the MAGI assay only detects first round of viral infection up to Tat expression. Therefore, it may be ideal for determination of accurate inhibitory effect compared to other assays that allow multiple replications.

the MFold program version 3.2 (http://frontend.bioinfo.rpi.edu/applications/mfold/) (Mathews et al., 1999; Zuker, 2003). The replication kinetics of HIV-1N43K-AAA and HIV-1N43K-AAG were comparable, in combination of L44L-CTG, however, that of HIV-1N43K-AAA was greater by the CHRA. It is possible that the nucleotide sequence itself may affect binding affinity of Rev to the RRE, although detailed mechanism of the difference between N43K-AAA and -AAG remains to be elucidated. Introduction of D36G to N43K-containing clones did not improve the replication kinetics of N43K-containing clones but restored their susceptibilities to T-20 (Table 1). These results indicate that synonymous mutations thus maintain HIV-1 replication.

A combination of primary mutations, namely Q40H and L45M (both ΔG values are 0.1 but in combination that is −4.5), which are complementarily located and stabilize stem III structure (Fig. 1B) and observed in vivo (Cabrera et al., 2006; Marcial et al., 2006; Mink et al., 2005; Xu et al., 2005), may alter the replication kinetics at either the nucleotide or amino acid level. Recent studies also highlight strong co-presence of Q40H and L45M in clinical isolates treated with T-20 (Svicher et al., 2008). These results sug-

Table 2
Effect of synonymous mutations on replication of HIV-1.

Mutation background	Order of replication
N43D	$HIV\text{-}1_{N43D/L44L\text{-}CUG} = HIV\text{-}1_{Q41Q\text{-}CAA/N43D} > HIV\text{-}1_{N43D} = HIV\text{-}1_{Q39Q\text{-}CAA/N43D}$
D36G/N43D	$HIV\text{-}1_{D36G/N43D/L44L\text{-}CUG} = HIV\text{-}1_{D36G/Q41Q\text{-}CAA/N43D} > HIV\text{-}1_{D36G/N43D} > HIV\text{-}1_{D36G/Q39Q\text{-}CAA/N43D}$
N43K	$HIV\text{-}1_{N43K\text{-}AAA/L44L\text{-}CUG} > HIV\text{-}1_{N43K\text{-}AAG/L44L\text{-}CUG} > HIV\text{-}1_{N43K\text{-}AAA} = HIV\text{-}1_{N43K\text{-}AAG}$
Synonymous mutations	$HIV\text{-}1_{L44L\text{-}CUG} = HIV\text{-}1_{Q41Q\text{-}CAA} > HIV\text{-}1_{WT} = HIV\text{-}1_{Q39Q\text{-}CAA}$

Competition of HIV-1 replication assay (CHRA) was performed in MT-2 cells. At least two independent CHRAs were performed.

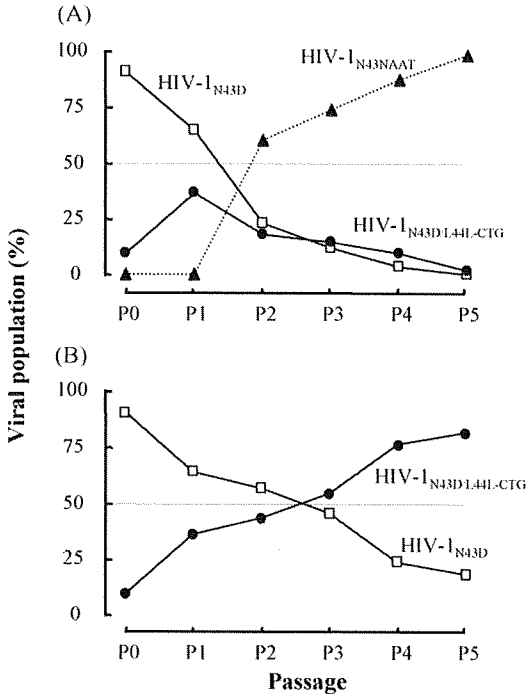

Fig. 2. Emergence of HIV-$1_{N43N\text{-}AAT}$ (HIV-1_{WT}) during CHRA for HIV-1_{N43D} and HIV-$1_{N43D/L44L\text{-}CTG}$ are shown. Open square, closed circle, and closed triangle represent HIV-1_{N43D}, HIV-$1_{N43D/L44L\text{-}CTG}$, and HIV-$1_{N43N\text{-}AAT}$, respectively. Absolute viral populations of each HIV-1s (A) and relative viral populations of HIV-1_{N43D} and HIV-$1_{N43D/L44L\text{-}CTG}$ (B) were shown.

gest that introduction of the primary mutations in the nucleotide level are affected by the RRE stability, indicating that amino acid and nucleotide substitutions in the gp41 and the RRE, respectively, co-operatively play a role.

3.4. *Effect of synonymous mutations*

As expected, the synonymous mutations (Q39Q-CAA, Q41Q-CAA, and L44L-CUG) solely affect viral replication but not T-20 susceptibility (0.7–2.6-fold in Table 1). They displayed an order of replication of HIV-1L44L-CUG = HIV-1Q41Q-CAA > HIV-1WT = HIV-1Q39Q-CAA, also demonstrating that only synonymous and complementary mutations, Q41Q-CAA and L44L-CTG, enhance replication kinetics. Finally, HIV-1L44L-UUA that is not detected in vivo was constructed and its replication kinetics was examined. As shown in Fig. 1, the third nucleotide for L44 raises the ΔG value, thus indicating that structure of the stem-loop III is unstable. The variants displayed impaired replication kinetics (Table 1). These results indicate that, in addition to the influence on gp41 function by amino acid substitutions, the structural stability of stem-loop III is one of the major determinants of the replication kinetics of mutated clones.

4. Discussion

This study demonstrated that synonymous mutations in the stem-loop III of RRE play an important role in the improvement of HIV-1 replication without affecting T-20 susceptibility. The structural stability of stem-loop III defined by ΔG value was strongly correlated with the replication kinetics ($R^2 = 0.76$, Fig. 1C), while the susceptibility, based on the EC_{50} value, was less ($R^2 < 0.3$ excluding clones that showed over 48-fold resistance, data not shown). Although it is likely that the nucleotide sequence of stem-loop III as well as the structural stability may also influence the RRE functions, including Rev binding, the current results indicate that the structural stability of RRE as well as gp41 amino acid substitutions seem to be a determinant for replication kinetics. At present, however, it is impossible to conclude that the pre-existence of such synonymous mutations in the RRE predicts on how T-20 resistance mutations are acquired.

Armand-Ugón et al initially isolated and reported resistance to C34 in vitro (Armand-Ugón et al., 2003), although we previously demonstrated that some of mutations for C34 resistance are involved in the RRE function as described (Nameki et al., 2005). The variants contained L33S or V38E mutations in the gp41 and both showed strong (more than 500-fold resistance) C34 resistance (Armand-Ugón et al., 2003). These mutations in the nucleotide level are also located in RRE (Fig. 1A); the nucleotide substitutions for L33S and V38E are located in the loop of stem IIB and the middle of stem IIC, respectively. Interestingly, V38E emerged in the HxB2-derived strain containing D36G polymorphism that stabilizes stem IIB structure, while L33S, which might have little effect on stem IIC stability due to its location, was observed in the NL4-3-derived resistant strain. These results also suggest that introduction of some mutations in the gp41 is restricted by RRE function. Armand-Ugón et al. (2003) failed to identify the secondary mutations for L33S or V38E. It is likely that the effect on RRE function may be tolerable for viral replication. Alternatively, relative short induction periods (maximum 17 passages) might also influence efficient introduction of the secondary mutations.

Functional analysis for Rev, RRE, and/or both seems to be important to reveal a detailed effect on viral replication. In this regard, we have previously demonstrated that effect of mutations for C34 resistance located in stem-loop II on binding of Rev to RRE was not apparent (less than 10% in the gel shift assay (Nameki et al., 2005)). It is possible that other factors including nuclear export and host factors, which may be influenced by the mutations, are involved in viral replication through interaction of Rev/RRE in HIV infected cells. Therefore, in the present study, we constructed an artificial mutant L44-TTA, which destabilizes or disrupts the stem III structure, and examined the effect on viral replication (Table 1). Replication of L44-TTA containing mutant showed much reduced replication kinetics even without gp41 amino acid substitutions, again indicating that stem III also plays an important role in viral replication.

So far, no information concerning Rev and Tat nucleotide substitutions is available in T-20 experienced patients. It is possible that the altered function of RRE may induce Rev mutation(s). In this regard, the entire sequence of Rev coding region of a C34 resistant variant was determined, however, no mutations were observed (Nameki et al., 2005). Most of the coding region of Rev also encodes Tat and gp41, thus indicating that Rev mutation(s) would alter these functions. This suggests that, even for single amino acid substitution, the genetic barrier for T-20 resistance seems to be relatively high when synonymous mutations are required to be introduced with the primary mutations and further fusion inhibitors that target the N-helical region thus appear to be promising.

In conclusion, this study provides valuable insight into the functional importance of RRE in HIV-1 with T-20 resistance for the replication kinetics. To reveal the function of gp41, experiments with artificial amino acid substitutions, *e.g.*, alanine scanning, which can be used to rapidly identify residues important for protein function by alanine substitution, should be carefully conducted. Further studies will reveal the functional significance of the RNA and protein function in this region.

Acknowledgements

HeLa-CD4-LTR-β-gal cells were kindly provided by Dr. M. Emerman through the AIDS Research and Reference Reagent Program,

Division of AIDS, National Institute of Allergy and Infectious Disease (Bethesda, MD). M.U., K.S., Y. Sakurai., and K.K. were supported by the 21st Century COE program of the Ministry of Education, Culture, Sports, Science, and Technology. This work was supported by grants for the promotion of AIDS Research from the Ministry of Health, Labor, and Welfare and Research for Health Sciences Focusing on Drug Innovation from The Japan Health Sciences Foundation (E.N.K., S.O., N.F., and M.M.).

References

Armand-Ugón, M., Gutiérrez, A., Clotet, B., Esté, J.A., 2003. HIV-1 resistance to the gp41-dependent fusion inhibitor C-34. Antiviral Res. 59, 137–142.

Bishop, K.N., Holmes, R.K., Sheehy, A.M., Davidson, N.O., Cho, S.J., Malim, M.H., 2004. Cytidine deamination of retroviral DNA by diverse APOBEC proteins. Curr. Biol. 14, 1392–1396.

Cabrera, C., Marfil, S., García, E., Martinez-Picado, J., Bonjoch, A., Bofill, M., Moreno, S., Ribera, E., Domingo, P., Clotet, B., Ruiz, L., 2006. Genetic evolution of gp41 reveals a highly exclusive relationship between codons 36, 38 and 43 in gp41 under long-term enfuvirtide-containing salvage regimen. AIDS 20, 2075–2080.

Fikkert, V., Cherepanov, P., Van Laethem, K., Hantson, A., Van Remoortel, B., Pannecouque, C., De Clercq, E., Debyser, Z., Vandamme, A.M., Witvrouw, M., 2002. env chimeric virus technology for evaluating human immunodeficiency virus susceptibility to entry inhibitors. Antimicrob. Agents Chemother. 46, 3954–3962.

Fung, H.B., Guo, Y., 2004. Enfuvirtide: a fusion inhibitor for the treatment of HIV infection. Clin. Ther. 26, 352–378.

Hachiya, A., Kodama, E.N., Sarafianos, S.G., Schuckmann, M.M., Sakagami, Y., Matsuoka, M., Takiguchi, M., Gatanaga, H., Oka, S., 2008. Amino acid mutation N348I in the connection subdomain of human immunodeficiency virus type 1 reverse transcriptase confers multiclass resistance to nucleoside and nonnucleoside reverse transcriptase inhibitors. J. Virol. 82, 3261–3270.

Harris, R.S., Bishop, K.N., Sheehy, A.M., Craig, H.M., Petersen-Mahrt, S.K., Watt, I.N., Neuberger, M.S., Malim, M.H., 2003. DNA deamination mediates innate immunity to retroviral infection. Cell 113, 803–809.

Kimpton, J., Emerman, M., 1992. Detection of replication-competent and pseudotyped human immunodeficiency virus with a sensitive cell line on the basis of activation of an integrated beta-galactosidase gene. J. Virol. 66, 2232–2239.

Kinomoto, M., Yokoyama, M., Sato, H., Kojima, A., Kurata, T., Ikuta, K., Sata, T., Tokunaga, K., 2005. Amino acid 36 in the human immunodeficiency virus type 1 gp41 ectodomain controls fusogenic activity: implications for the molecular mechanism of viral escape from a fusion inhibitor. J. Virol. 79, 5996–6004.

Kodama, E.I., Kohgo, S., Kitano, K., Machida, H., Gatanaga, H., Shigeta, S., Matsuoka, M., Ohrui, H., Mitsuya, H., 2001. 4′-Ethynyl nucleoside analogs: potent inhibitors of multidrug-resistant human immunodeficiency virus variants in vitro. Antimicrob. Agents Chemother. 45, 1539–1546.

Labrosse, B., Morand-Joubert, L., Goubard, A., Rochas, S., Labernardiére, J.L., Pacanowski, J., Meynard, J.L., Hance, A.J., Clavel, F., Mammano, F., 2006. Role of the envelope genetic context in the development of enfuvirtide resistance in human immunodeficiency virus type 1-infected patients. J. Virol. 80, 8807–8819.

Lalezari, J.P., Henry, K., O'Hearn, M., Montaner, J.S., Piliero, P.J., Trottier, B., Walmsley, S., Cohen, C., Kuritzkes, D.R., Eron Jr., J.J., Chung, J., DeMasi, R., Donatacci, L., Drobnes, C., Delehanty, J., Salgo, M., 2003. Enfuvirtide, an HIV-1 fusion inhibitor, for drug-resistant HIV infection in North and South America. N. Engl. J. Med. 348, 2175–2185.

Lazzarin, A., Clotet, B., Cooper, D., Reynes, J., Arastéh, K., Nelson, M., Katlama, C., Stellbrink, H.J., Delfraissy, J.F., Lange, J., Huson, L., DeMasi, R., Wat, C., Delehanty, J., Drobnes, C., Salgo, M., 2003. Efficacy of enfuvirtide in patients infected with drug-resistant HIV-1 in Europe and Australia. N. Engl. J. Med. 348, 2186–2195.

Liddament, M.T., Brown, W.L., Schumacher, A.J., Harris, R.S., 2004. APOBEC3F properties and hypermutation preferences indicate activity against HIV-1 in vivo. Curr. Biol. 14, 1385–1391.

Lu, J., Deeks, S.G., Hoh, R., Beatty, G., Kuritzkes, B.A., Martin, J.N., Kuritzkes, D.R., 2006. Rapid emergence of enfuvirtide resistance in HIV-1-infected patients: results of a clonal analysis. J. Acquir. Immune Defic. Syndr. 43, 60–64.

Lu, J., Sista, P., Giguel, F., Greenberg, M., Kuritzkes, D.R., 2004. Relative replicative fitness of human immunodeficiency virus type 1 mutants resistant to enfuvirtide (T-20). J. Virol. 78, 4628–4637.

Maeda, Y., Venzon, D.J., Mitsuya, H., 1998. Altered drug sensitivity, fitness, and evolution of human immunodeficiency virus type 1 with pol gene mutations conferring multi-dideoxynucleoside resistance. J. Infect. Dis. 177, 1207–1213.

Manfredi, R., Sabbatani, S., 2006. A novel antiretroviral class (fusion inhibitors) in the management of HIV infection. Present features and future perspectives of enfuvirtide (T-20). Curr. Med. Chem. 13, 2369–2384.

Mangeat, B., Turelli, P., Caron, G., Friedli, M., Perrin, L., Trono, D., 2003. Broad antiretroviral defence by human APOBEC3G through lethal editing of nascent reverse transcripts. Nature 424, 99–103.

Marcelin, A.G., Reynes, J., Yerly, S., Ktorza, N., Segondy, M., Piot, J.C., Delfraissy, J.F., Kaiser, L., Perrin, L., Katlama, C., Calvez, V., 2004. Characterization of genotypic determinants in HR-1 and HR-2 gp41 domains in individuals with persistent HIV viraemia under T-20. AIDS 18, 1340–1342.

Marcial, M., Lu, J., Deeks, S.G., Ziermann, R., Kuritzkes, D.R., 2006. Performance of human immunodeficiency virus type 1 gp41 assays for detecting enfuvirtide (T-20) resistance mutations. J. Clin. Microbiol. 44, 3384–3387.

Mathews, D.H., Sabina, J., Zuker, M., Turner, D.H., 1999. Expanded sequence dependence of thermodynamic parameters improves prediction of RNA secondary structure. J. Mol. Biol. 288, 911–940.

Menzo, S., Castagna, A., Monachetti, A., Hasson, H., Danise, A., Carini, E., Bagnarelli, P., Lazzarin, A., Clementi, M., 2004. Genotype and phenotype patterns of human immunodeficiency virus type 1 resistance to enfuvirtide during long-term treatment. Antimicrob. Agents Chemother. 48, 3253–3259.

Mink, M., Mosier, S.M., Janumpalli, S., Davison, D., Jin, L., Melby, T., Sista, P., Erickson, J., Lambert, D., Stanfield-Oakley, S.A., Salgo, M., Cammack, N., Matthews, T., Greenberg, M.L., 2005. Impact of human immunodeficiency virus type 1 gp41 amino acid substitutions selected during enfuvirtide treatment on gp41 binding and antiviral potency of enfuvirtide in vitro. J. Virol. 79, 12447–12454.

Morozov, V.A., Morozov, A.V., Schürmann, D., Jessen, H., Kücherer, C., 2007. Transmembrane protein polymorphisms and resistance to T-20 (Enfuvirtide, Fuzeon) in HIV-1 infected therapy-naive seroconverters and AIDS patients under HAART-T-20 therapy. Virus Genes 35, 167–174.

Nameki, D., Kodama, E., Ikeuchi, M., Mabuchi, N., Otaka, A., Tamamura, H., Ohno, M., Fujii, N., Matsuoka, M., 2005. Mutations conferring resistance to human immunodeficiency virus type 1 fusion inhibitors are restricted by gp41 and Rev-responsive element functions. J. Virol. 79, 764–770.

Olsen, H.S., Nelbock, P., Cochrane, A.W., Rosen, C.A., 1990. Secondary structure is the major determinant for interaction of HIV rev protein with RNA. Science 247, 845–848.

Otaka, A., Nakamura, M., Nameki, D., Kodama, E., Uchiyama, S., Nakamura, S., Nakano, H., Tamamura, H., Kobayashi, Y., Matsuoka, M., Fujii, N., 2002. Remodeling of gp41-C34 peptide leads to highly effective inhibitors of the fusion of HIV-1 with target cells. Angew. Chem. Int. Ed. Engl. 41, 2937–2940.

Pérez-Alvarez, L., Carmona, R., Ocampo, A., Asorey, A., Miralles, C., Pérez de Castro, S., Pinilla, M., Contreras, G., Taboada, J.A., Nájera, R., 2006. Long-term monitoring of genotypic and phenotypic resistance to T20 in treated patients infected with HIV-1. J. Med. Virol. 78, 141–147.

Poveda, E., Rodés, B., Toro, C., Martín-Carbonero, L., Gonzalez-Lahoz, J., Soriano, V., 2002. Evolution of the gp41 env region in HIV-infected patients receiving T-20, a fusion inhibitor. AIDS 16, 1959–1961.

Si-Mohamed, A., Piketty, C., Tisserand, P., LeGoff, J., Weiss, L., Charpentier, C., Kazatchkine, M.D., Bélec, L., 2007. Increased polymorphism in the HR-1 gp41 env gene encoding the enfuvirtide (T-20) target in HIV-1 variants harboring multiple antiretroviral drug resistance mutations in the pol gene. J. Acquir. Immune Defic. Syndr. 44, 1–5.

Sista, P.R., Melby, T., Davison, D., Jin, L., Mosier, S., Mink, M., Nelson, E.L., DeMasi, R., Cammack, N., Salgo, M.P., Matthews, T.J., Greenberg, M.L., 2004. Characterization of determinants of genotypic and phenotypic resistance to enfuvirtide in baseline and on-treatment HIV-1 isolates. AIDS 18, 1787–1794.

Su, C., Melby, T., DeMasi, R., Ravindran, P., Heilek-Snyder, G., 2006. Genotypic changes in human immunodeficiency virus type 1 envelope glycoproteins on treatment with the fusion inhibitor enfuvirtide and their influence on changes in drug susceptibility in vitro. J. Clin. Virol. 36, 249–257.

Svicher, V., Aquaro, S., D'Arrigo, R., Artese, A., Dimonte, S., Alcaro, S., Santoro, M.M., Di Perri, G., Caputo, S.L., Bellagamba, R., Zaccarelli, M., Visco-Comandini, U., Antinori, A., Narciso, P., Ceccherini-Silberstein, F., Perno, C.F., 2008. Specific enfuvirtide-associated mutational pathways in HIV-1 gp41 are significantly correlated with an increase in CD4(+) cell count, despite virological failure. J. Infect. Dis. 197, 1408–1418.

Wei, X., Decker, J.M., Liu, H., Zhang, Z., Arani, R.B., Kilby, J.M., Saag, M.S., Wu, X., Shaw, G.M., Kappes, J.C., 2002. Emergence of resistant human immunodeficiency virus type 1 in patients receiving fusion inhibitor (T-20) monotherapy. Antimicrob. Agents Chemother. 46, 1896–1905.

Wiegand, H.L., Doehle, B.P., Bogerd, H.P., Cullen, B.R., 2004. A second human antiretroviral factor, APOBEC3F, is suppressed by the HIV-1 and HIV-2 Vif proteins. EMBO J. 23, 2451–2458.

Xu, L., Pozniak, A., Wildfire, A., Stanfield-Oakley, S.A., Mosier, S.M., Ratcliffe, D., Workman, J., Joall, A., Myers, R., Smit, E., Cane, P.A., Greenberg, M.L., Pillay, D., 2005. Emergence and evolution of enfuvirtide resistance following long-term therapy involves heptad repeat 2 mutations within gp41. Antimicrob. Agents Chemother. 49, 1113–1119.

Zapp, M.L., Green, M.R., 1989. Sequence-specific RNA binding by the HIV-1 Rev protein. Nature 342, 714–716.

Zhang, H., Yang, B., Pomerantz, R.J., Zhang, C., Arunachalam, S.C., Gao, L., 2003. The cytidine deaminase CEM15 induces hypermutation in newly synthesized HIV-1 DNA. Nature 424, 94–98.

Zuker, M., 2003. Mfold web server for nucleic acid folding and hybridization prediction. Nucleic Acids Res. 31, 3406–3415.

Peptide bond mimicry by (*E*)-alkene and (*Z*)-fluoroalkene peptide isosteres: synthesis and bioevaluation of α-helical anti-HIV peptide analogues†

Shinya Oishi,*[a] Hirotaka Kamitani,[a] Yasuyo Kodera,[a] Kentaro Watanabe,[a] Kazuya Kobayashi,[a] Tetsuo Narumi,[a] Kenji Tomita,[a] Hiroaki Ohno,[a] Takeshi Naito,[b] Eiichi Kodama,[b] Masao Matsuoka[b] and Nobutaka Fujii*[a]

Received 22nd April 2009, Accepted 30th April 2009
First published as an Advance Article on the web 4th June 2009
DOI: 10.1039/b907983a

The α-helix structures of the anti-HIV fusion inhibitory peptides are stabilized by the amino acid sequence and by intrachain hydrogen bonds. The study of peptide analogues using (*E*)-alkene and (*Z*)-fluoroalkene dipeptide isosteres demonstrated the substantial, yet position-dependent, contribution of hydrogen bonds to the α-helix stability and anti-HIV bioactivity.

Introduction

The α-helix represents one of the largest classes of secondary structure elements found in protein and peptide structures.[1] The cylindrical structures are stabilized by intrachain hydrogen bond (H-bond) networks which are formed between the C=O of residue *i* and the amide N–H of the *i*+4 residue to generate 13-membered pseudocyclic structures. The functional and/or interactive surface(s) of the α-helix are revealed by the arrangement of the distribution residues in the linear sequence upon folding.

In order to stabilize the α-helix structure of bioactive peptides, there are two possible approaches: (1) bridging side-chains by covalent or non-covalent bond(s) or (2) mimicking intrachain H-bond(s).[2] Recently, we reported a novel design concept of fusion inhibitory peptides active against HIV-1 by utilizing an X-EE-XX-KK motif (X: original residue; E: glutamic acid; K: lysine).[3,4] This motif contributes to the stabilization of the bioactive α-helix conformation by forming two potential salt bridges between Glu and Lys side-chains without altering the location of residues that form the interactive surface with the viral protein gp41.[4c] The peptides, named SC35EK and T-20EK, exhibit highly potent anti-HIV activity by inhibition of the rearrangement of HIV-1 gp41 that facilitates fusion between the host cellular and viral membranes. In addition, a structure–activity relationship study identified a novel amphiphilic peptide, SC29EK, with a minimal sequence for anti-HIV activity.[5] In light of its high potency of SC29EK, it was of interest to estimate the effect of intrachain H-bond(s) on α-helix stabilization in the presence of the X-EE-XX-KK motifs. Accordingly, efforts herein have been undertaken to comparatively evaluate the anti-HIV activity and biophysical properties of SC29EK analogues containing peptide bond mimetics.

(*E*)-Alkene dipeptide isostere (EADI) **1** and (*Z*)-fluoroalkene dipeptide isostere (FADI) **2** of Lys-Lys were chosen as planar peptide bond surrogates for positional scanning of each Lys-Lys dipeptide in four repeat motifs (Fig. 1).[6] Two potential H-bonds may be missing when replacing the peptide bond in Lys-Lys with the olefin congeners: (1) between the C=O of the first Lys (*i*) and the N–H of the downward Glu (*i*+4), (2) between the N–H of the second Lys (*i*+1) and the C=O of the upward Glu (*i*−3) (Fig. 1). In the case of FADI substitution, the presence of the first H-bond was expected, because of the potential ability of a fluorine atom to act as a H-bond acceptor.[7]

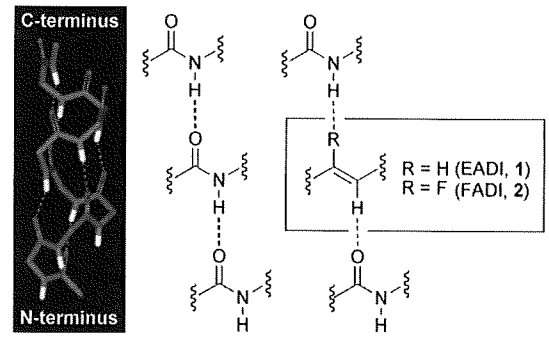

Fig. 1 Structures of (*E*)-alkene and (*Z*)-fluoroalkene dipeptide isosteres and the potential mimicry of H-bonds stabilizing the α-helix structure.

Results and discussion

Lys-Lys EADI[8] and FADI[9] were prepared by the established procedures shown in Schemes 1 and 2, respectively. Briefly, allyl alcohol **3**[10] derived from a protected amino acid was converted into Ns-amide **4**. Aziridination of **4** by the Mitsunobu reaction followed by C-1 elongation afforded the β-aziridinyl-α,β-unsaturated ester **6**. Organocopper-mediated alkylation of **6** provided an α-alkyl adduct **7** regio- and stereoselectively. Subsequent functional group manipulations generated the expected Fmoc-protected EADI **10**.

FADI synthesis began with mono-TBS-protected 1,5-pentanediol **11**. Rh-catalyzed Reformatsky–Honda reaction[11] of the corresponding aldehyde gave α,α-difluoro-β-amino ester **12**. The simultaneous hydrogenolysis and Boc protection followed by C-2 elongation using the Horner–Wadsworth–Emmons reaction produced a key γ,γ-difluoro-α,β-enoyl sultam **14**. One-pot reduction/asymmetric alkylation *via* transmetalation with allyl bromide formed the FADI scaffold **15**. Selective

[a]*Graduate School of Pharmaceutical Sciences, Kyoto University, Sakyo-ku, Kyoto, 606-8501, Japan. E-mail: soishi@pharm.kyoto-u.ac.jp, nfujii@pharm.kyoto-u.ac.jp; Fax: +81-75-753-4570; Tel: +81-75-753-4551*
[b]*Laboratory of Virus Control, Institute for Virus Research, Kyoto University, Sakyo-ku, Kyoto, 606-8507, Japan*

† Electronic supplementary information (ESI) available: Additional experimental procedures, NMR spectra and HPLC charts. See DOI: 10.1039/b907983a

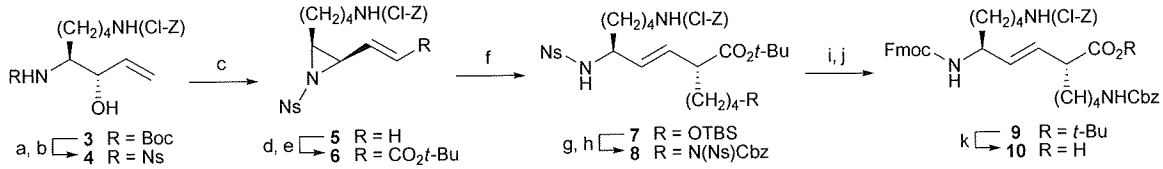

Scheme 1 Synthesis of the Lys-Lys-type alkene dipeptide isostere. *Reagents and conditions*: (a) 4 N HCl/dioxane; (b) NsCl, 2,4,6-collidine, $CHCl_3$, 65% (2 steps); (c) DIAD, PPh_3, THF/toluene, 0 °C, 84%; (d) O_3, AcOEt, −78 °C, then Me_2S; (e) $(EtO)_2P(O)CH_2CO_2t$-Bu, LiCl, DIEA, CH_3CN, 0 °C, 46% (2 steps); (f) $TBSO(CH_2)_4I$, *t*-BuLi, CuCN, LiCl, *n*-pentane/Et_2O/THF, −78 °C, 60%; (g) H_2SiF_6 aq., CH_3CN/CH_3OH, 0 °C; (h) CbzNHNs, PPh_3, DIAD, THF/toluene, 81% (2 steps); (i) PhSH, K_2CO_3, DMF; (j) Fmoc-OSu, Et_3N, DMF, 84% (2 steps); (k) 4 N HCl/dioxane, 96%.

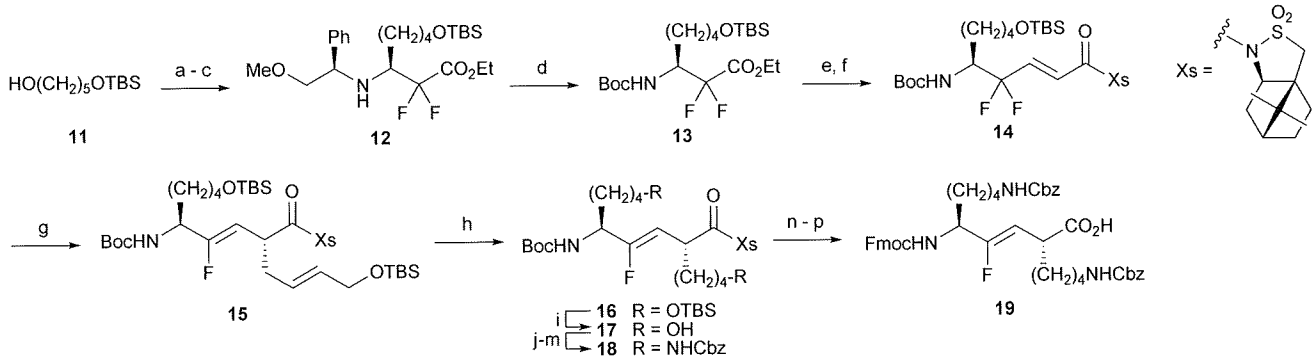

Scheme 2 Synthesis of the Lys-Lys-type fluoroalkene dipeptide isostere. *Reagents and conditions*: (a) DMSO, $(COCl)_2$, Et_3N, CH_2Cl_2, −78 °C; (b) (*R*)-2-methoxy-1-phenylethylamine, 3 Å MS, THF, 0 °C; (c) $BrCF_2CO_2Et$, $RhCl(PPh_3)_3$, Et_2Zn, 0 °C, 43% (3 steps); (d) $Pd(OH)_2$, H_2, Boc_2O, EtOH, 87%; (e) DIBAL-H, CH_2Cl_2/toluene −78 °C; (f) $(EtO)_2P(O)CH_2COXs$, LiCl, DIEA, CH_3CN, 0 °C, 87% (2 steps); (g) $Me_2CuLi{\cdot}LiI$, THF/Et_2O, −78 °C, then HMPA, then Ph_3SnCl, −78 °C to −40 °C, then $BrCH_2$–(*E*)-CH=CH–CH_2OTBS, −40 °C, 78%; (h) 4.5% Pd/C(en), EtOH, H_2; (i) aq. H_2SiF_6, CH_3CN/CH_3OH, 78% (2 steps); (j) TsCl, Et_3N, CH_2Cl_2; (k) NaN_3, DMF; (l) PPh_3, THF/H_2O; (m) Cbz-OSu, Et_3N, DMF, 65% (4 steps); (n) 1 N LiOH, 50% H_2O_2, THF/H_2O; (o) TFA, CH_2Cl_2; (p) Fmoc-OSu, Et_3N, MeCN/DMF/H_2O, 64% (3 steps).

hydrogenation in the presence of Pd/C(en)[12] and step-wise modifications afforded the Fmoc-protected FADI **19**. The resulting isosteres **10** and **19** were incorporated into the KK dipeptide of SC29EK sequence by standard Fmoc-based solid-phase peptide synthesis.

Anti-HIV activities of the isostere-containing peptides **20E–23E** and **20F–23F** were examined using the MAGI assay (Table 1). Substitutions of the first and second N-terminal Lys-Lys dipeptides with EADI (**20E** and **21E**) resulted in the loss of the anti-HIV activity (EC_{50} >10 μM). In contrast, the FADI congeners exhibited weak or moderate anti-HIV activities (**20F**: EC_{50} = 5.2 μM; **21F**: EC_{50} = 599 nM). Both EADI and FADI analogues with substitution at the third Lys-Lys showed slightly lower anti-HIV potency than wild-type C29[5] without the α-helix inducible XEEXXKK motifs (**22E**: EC_{50} = 865 nM; **22F**: EC_{50} = 663 nM). The best peptide analogues were obtained by replacement of the C-terminal Lys-Lys with the isosteres (**23E**: EC_{50} = 43 nM; **23F**: EC_{50} = 37 nM); however, the potency was lower than the original SC29EK peptide (EC_{50} = 2.2 nM). Similar bioactivities of peptide **20E–23E** and **20F–23F** were also observed against the other HIV-1 strains (Table 2). These observations suggest that all the peptide bonds within the Lys-Lys and the related H-bonding are essential for the potent anti-HIV activity of SC29EK.

The α-helix properties of these peptides were determined by circular dichroism (CD) analysis (Fig. 2a,b). The stable α-helix

Table 1 Sequences and anti-HIV activities of C29 and its derivatives and T_m values of the mixture with N36

	EADI analogues **E**		FADI analogues **F**	
Sequence[a]	EC_{50} (nM)[b]	T_m (°C)[c]	EC_{50} (nM)[b]	T_m (°C)[c]
WMEWDREINNYTSLIHSLIEESQNQQEKN C29	308 ± 144	51.7	—	—
WEEWDKKIEEYTKKIEELIKKSEEQQKKN SC29EK	2.2 ± 0.2	67.4	—	—
WEEWDKKIEEYTKKIEELIKKSEEQQKKN **20E/20F**	>10000	43.9	5220 ± 202	44.1
WEEWDKKIEEYTKKIEELIKKSEEQQKKN **21E/21F**	>10000	40.1	599 ± 96	49.5
WEEWDKKIEEYTKKIEELIKKSEEQQKKN **22E/22F**	865 ± 317	62.2	663 ± 242	60.9
WEEWDKKIEEYTKKIEELIKKSEEQQKKN **23E/23F**	43 ± 7	64.1	37 ± 6	64.8

[a] The underlined KK dipeptide indicates the position of the dipeptide isostere. [b] EC_{50} was determined as the concentration that blocked HIV-1 (NL4–3 strain) replication by 50%. [c] T_m values were defined by the midpoint of the thermal unfolding transition state as determined from $[\theta]_{222}$ readings.

Table 2 Anti-HIV activities of C29 and its derivatives against three HIV-1 strains

Peptides	EC_{50} (nM)[a]		
	NL4–3	IIIB	Ba-L
C29	308 ± 144	396 ± 83	42 ± 8
SC29EK	2.2 ± 0.2	6.5 ± 0.9	1.9 ± 0.2
20E	>10000	>10000	>10000
20F	5220 ± 202	>10000	5580 ± 1920
21E	>10000	>10000	>10000
21F	599 ± 96	3010 ± 554	600 ± 302
22E	865 ± 317	5110 ± 2,750	2630 ± 386
22F	663 ± 242	2200 ± 712	527 ± 95
23E	37 ± 6	153 ± 27	33 ± 2
23F	43 ± 7	237 ± 16	51 ± 7

[a] EC_{50} is the concentration that blocks HIV-1 replication by 50%.

structure of SC29EK was disrupted by a single substitution of the second or third Lys-Lys peptide bond with the isosteres in **21E/21F** and **22E/22F**. This suggests that the contribution of the H-bonds to the stability of the α-helix is likely to be superior to the multiple introductions of the X-EE-XX-KK motifs at these positions. Conversely, the effects of N- and C-terminal substitution were less significant as observed in **20E/20F** and **23E/23F**. This may be rationalized by the fact that these peptide bonds of SC29EK are positioned at the edge of the helix and that C-terminal Lys-Lys is involved in only upward H-bonding through the donor N–H moiety. CD spectra of SC29EK analogues in the presence of an interactive counterpart N36 indicated the formation of stable six-helix coiled-coil structures (Fig. 2c,d).[13] This observation supports the concept that SC29EK analogues exert their anti-HIV activity by inhibiting the folding process of the HIV-1 envelop protein gp41.

Binding affinity of SC29EK analogues to a viral protein was determined by the thermal stability of the six-helix complexes formed between SC29EK and N36 peptides. The melting temperature (T_m), representing 50% disruption of the six-helix bundle, was comparatively evaluated by monitoring the change in the circular dichroism signal at 222 nm as a function of increasing temperature (Table 1). The complexes involving peptides **20E/20F** and **21E/21F** showed significantly lower thermal stability, which correlates with the observed absent or low anti-HIV activities of these peptides. In contrast, potent analogues **23E/23F** form stable complexes with N36 with T_m values comparable to the value measured for SC29EK (**23E**: T_m = 64.1 °C; **23F**: T_m = 64.8 °C). The N-terminal tryptophan-rich domain (WRD) of inhibitory peptides such as C34 is essential for binding to the cavity formed by the N36 coiled-coil.[11] H-Bonds linked by the first and second Lys-Lys peptide bonds in SC29EK would reinforce the arrangement of these tryptophans. Interestingly, less potent anti-HIV activity of peptide **22E/22F** was observed compared with C29, whereas the complexes with N36 showed higher thermal stability. This result suggests that the loss of crucial H-bonds could reduce the anti-HIV activity, even though the X-EE-XX-KK motifs apparently aid the conformational stability of the six-helix bundle.

In terms of the mimicking ability of the two-peptide-bond isosteres, FADI peptides **20F–23F** exhibited slightly more potent anti-HIV activity and formed more stable complexes with N36 (except for **22F**). Although a fluoroalkene with a large dipole moment imperfectly reproduces the H-bonds needed for α-helix stabilization, FADI is an appropriate peptide bond surrogate to investigate structural requirements in bioactive peptides.

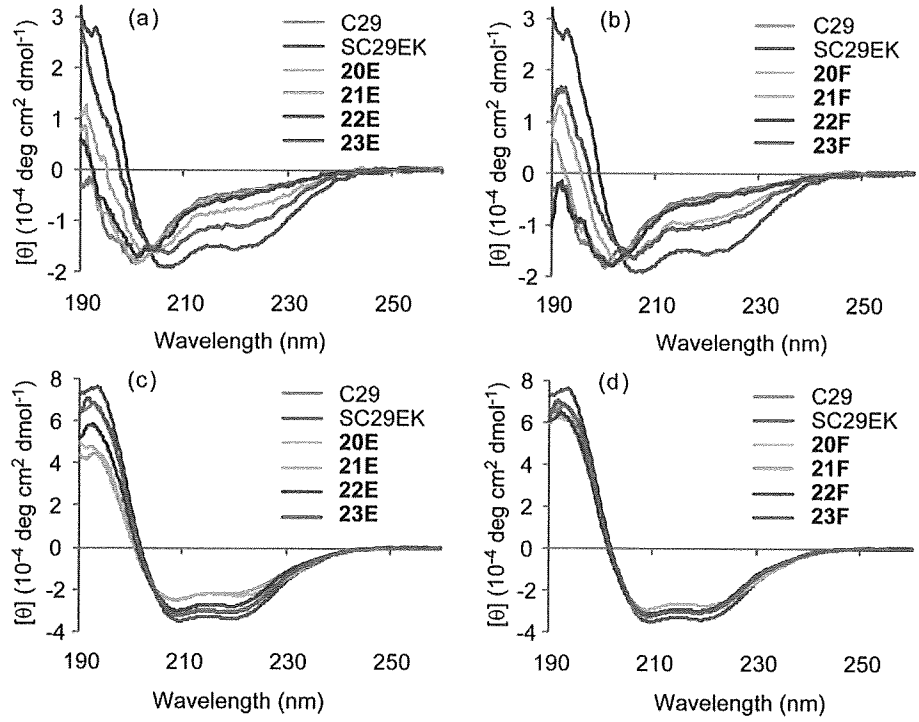

Fig. 2 CD spectra of EADI- and FADI-containing SC29EK analogues in the absence (a,b) and presence (c,d) of N36.

Conclusions

The effects of H-bonds on the stability of the α-helix of an HIV-1 fusion inhibitor were investigated by positional-scanning of the Lys-Lys dipeptides using EADI and FADI. As demonstrated by CD analysis of the SC29EK analogues, H-bonds in the middle of the sequence contribute significantly to the stabilization of the α-helix. In contrast, the effect of H-bonds on the anti-HIV activity of the peptides depends on the distance from the crucial interactive domain. As such, we have shown that EADI and FADI can be used for conformational evaluation of bioactive and/or functional α-helical peptides.

Experimental section

Synthesis

***tert*-Butyl (2*R*,5*S*,3*E*)-2-[4-(*tert*-butyldimethylsiloxy)butyl]-9-[*N*-(2-chlorobenzyloxycarbonyl)amino]-5-[*N*-(2-nitrophenylsulfonyl)amino]non-3-enoate (7).** To a stirred solution of TBSO-$(CH_2)_4$I (236 mg, 0.75 mmol) in dry Et_2O (0.5 cm^3), was added dropwise 1.59 M *t*-BuLi in Et_2O solution (1.0 cm^3, 1.58 mmol) under Ar at −78 °C. After being stirred at this temperature for 30 min, the mixture was stirred at 0 °C for 30 min. To a stirred solution of CuCN (61 mg, 0.61 mmol) and LiCl (52 mg, 1.23 mmol) in dry THF (0.8 cm^3), was added dropwise the above 0.5 M TBSO$(CH_2)_4$Li in THF solution (1.2 cm^3) under Ar at −78 °C, and the mixture was stirred at 0 °C for 10 min. A solution of aziridinyl enoate **6** (91 mg, 0.15 mmol) in dry THF (1.0 cm^3) was added dropwise to the above mixture at −78 °C with stirring, and the stirring was continued for 1.5 h followed by quenching with saturated NH_4Cl/28% NH_4OH solution (1/1, 2.0 cm^3). The mixture was washed with H_2O and brine and dried over $MgSO_4$. Concentration under reduced pressure followed by flash chromatography over silica gel with *n*-hexane-EtOAc (3:1) gave the title compound **7** (72 mg, 60%) as a colorless oil; $[\alpha]^{23}_D$ −73.2 (*c* 0.87 in $CHCl_3$); ν_{max}/cm^{-1} 3349 (NHCO), 1725 (CO); δ_H (500 MHz; $CDCl_3$) 0.04 (6H, s), 0.89 (9H, s), 1.08–1.64 (21H, m), 2.64 (1H, dt, *J* 8.0 and 6.3), 3.07–3.21 (2H, m), 3.55 (2H, t, *J* 6.3), 3.86–3.96 (1H, m), 4.92 (1H, br s), 5.21 (2H, s), 5.26 (1H, dd, *J* 15.5 and 7.5), 5.39 (1H, d, *J* 8.0), 5.40 (1H, dd, *J* 15.5 and 8.0), 7.22–7.30 (2H, m), 7.37 (1H, dd, *J* 5.7 and 2.3), 7.42 (1H, dd, *J* 5.7 and 2.3), 7.65–7.74 (2H, m), 7.83 (1H, dd, *J* 6.9 and 2.3), 8.09 (1H, dd, *J* 6.9 and 2.3); δ_C (100 MHz; $CDCl_3$) −5.3 (2C), 18.3, 22.5, 23.3, 25.9, 28.0 (3C), 29.3 (3C), 32.3, 32.6, 35.4, 40.6, 49.3, 56.7, 62.8, 63.9, 80.6, 125.3, 126.9, 129.3, 129.5, 129.8, 130.9 (2C), 131.2, 132.8, 133.3, 133.5, 134.3, 135.1, 147.8, 156.2, 172.8; *m/z* (FAB) 782.3246 ([M + H]$^+$, $C_{37}H_{57}ClN_3O_9SSi$ requires 782.3273).

(2*R*,5*S*,3*E*)-2-{4-[*N*-(*tert*-Butoxycarbonyl)amino]butyl}-9-[*N*-(2-chlorobenzyloxycarbonyl)amino]-5-[*N*-(9-fluorenylmethoxycarbonyl)amino]non-3-enoic acid (10). To the Fmoc-protected amine **9** (435 mg, 0.52 mmol) was added 4 N HCl/dioxane (5.0 cm^3) at 0 °C, and the mixture was stirred for 20 h at room temperature. Concentration under reduced pressure followed by flash chromatography over silica gel with *n*-hexane-EtOAc (1:1) gave the title compound **10** (391 mg, 96%) as a semisolid; $[\alpha]^{22}_D$ −18.0 (*c* 0.87 in $CHCl_3$); ν_{max}/cm^{-1} 3324 (NHCO), 1703 (CO); δ_H (500 MHz; $CDCl_3$) 1.09–1.81 (12H, m), 2.85–3.01 (1H, m), 3.03–3.21 (4H, m), 4.01–4.21 (2H, m), 4.30–4.54 (2H, m), 4.81–5.26 (6H, m), 5.30–5.81 (3H, m), 7.19–7.41 (13H, m), 7.52–7.59 (2H, m), 7.74 (2H, d, *J* 7.5); δ_C (125 MHz; $CDCl_3$) 22.5, 24.0, 29.2, 29.3, 31.5, 34.3, 40.6 (2C), 47.1, 48.4, 52.3, 63.7, 66.4 (2C), 119.8 (2C), 124.9 (2C), 126.7 (2C), 126.9 (2C), 127.5 (2C), 127.7, 127.9, 128.3, 129.2 (2C), 129.3 (2C), 129.5, 133.3, 134.2, 136.5, 141.1, 143.7 (2C), 143.8 (2C), 155.8, 156.3, 156.4, 178.0; *m/z* (FAB) 782.3201 ([M + H]$^+$, $C_{44}H_{49}ClN_3O_8$ requires 782.3208).

(2*R*,5*S*,3*Z*)-5-[*N*-(*tert*-Butoxycarbonyl)amino]-2-[(*E*)-4-(*tert*-butyldimethylsiloxy)but-2-enyl]-9-(*tert*-butyldimethylsiloxy)-4-fluoronon-3-enoyl (*S*)-sultam (15). To a suspension of CuI (180 mg, 0.94 mmol) in THF (4.8 cm^3) at −78 °C under argon was added dropwise a solution of MeLi·LiBr complex in Et_2O (1.5 M, 1.3 cm^3, 1.89 mmol), and the mixture was stirred for 10 min at 0 °C. To the solution of the above organocopper reagent at −78 °C was added dropwise a solution of the *N*-enoyl sultam **14** (150 mg, 0.24 mmol) in THF (4.8 cm^3). The mixture was stirred for 30 min at −78 °C and HMPA (0.66 cm^3, 3.78 mmol) was added dropwise to the mixture. After stirring for 30 min at −78 °C, a solution of triphenyltin chloride (182 mg, 0.47 mmol) in THF (3.0 cm^3) was added dropwise, and the mixture was then stirred for 30 min at −40 °C. (*E*)-(4-Bromobut-2-enyloxy)(*tert*-butyl)dimethylsilane (501 mg, 1.89 mmol) in THF (3.0 cm^3) was added dropwise and the mixture was stirred for 20 h at −40 °C. The reaction was quenched at −40 °C by addition of a saturated NH_4Cl/28% NH_4OH solution (1/1, 6.0 cm^3) and the mixture was stirred at room temperature for additional 30 min. The mixture was extracted with Et_2O and the extract was washed with brine and dried over $MgSO_4$. Concentration under reduced pressure followed by flash chromatography over silica gel with *n*-hexane-EtOAc (5:1) gave the title compound **15** (148 mg, 78% yield) as a colorless oil; $[\alpha]^{25}_D$ −47.1 (*c* 1.00 in $CHCl_3$); ν_{max}/cm^{-1} 3317 (NHCO), 1693 (CO); δ_H (500 MHz; $CDCl_3$) 0.03 (6H, s), 0.04 (6H, s), 0.88 (9H, s), 0.89 (9H, s), 0.96 (3H, s), 1.15 (3H, s), 1.24–1.64 (17H, m), 1.83–1.91 (3H, m), 2.02–2.05 (2H, m), 2.33–2.37 (1H, m), 2.51–2.55 (1H, m), 3.41 (1H, d, *J* 13.7), 3.49 (1H, d, *J* 13.7), 3.58 (2H, t, *J* 6.3), 3.86 (1H, t, *J* 6.3), 4.06 (2H, d, *J* 3.4), 4.12–4.21 (2H, m), 4.60–4.72 (1H, m), 4.97 (1H, dd, *J* 36.7 and 8.6), 5.58 (2H, m); δ_C (125 MHz; $CDCl_3$) −5.3 (4C), 18.2, 18.3, 19.8, 20.7, 21.9, 25.9 (6C), 26.4, 28.3 (3C), 32.2, 32.3, 32.8, 36.9, 38.3, 41.0, 44.6, 47.6, 48.2, 51.6 (d, *J* 27.6), 53.0, 62.8, 63.5, 65.1, 79.4, 103.3 (d, *J* 12.0), 125.9, 132.7, 154.8, 158.6 (d, *J* 261.5) 172.2; δ_F (470 MHz; $CDCl_3$) −119.1—119.8 (m); *m/z* (FAB) 801.4732 ([M + H]$^+$, $C_{40}H_{74}FN_2O_7SSi_2$ requires 801.4739).

(2*R*,5*S*,3*Z*)-2-{4-[*N*-(Benzyloxycarbonyl)amino]butyl}-9-[*N*-(benzyloxycarbonyl)amino]-5-[*N*-(9-fluorenylmethoxycarbonyl)-amino]-4-fluoronon-3-enoic acid (19). To a solution of the sultam **18** (376 mg, 0.34 mmol) and aqueous 50% H_2O_2 (0.12 cm^3, 1.75 mmol) in THF/H_2O (5/1, 6.0 cm^3) at 0 °C was added aqueous 1 N LiOH (0.67 cm^3, 0.67 mmol), and the mixture was stirred at room temperature for 2 h. After being diluted with EtOAc (20 cm^3), the mixture was washed with 0.1 N HCl and dried over $MgSO_4$. Concentration under reduced pressure gave the corresponding acid, which was used in the next reaction without purification. To a solution of the above acid in CH_2Cl_2 (15 cm^3) at 0 °C was added TFA (4.0 cm^3), and the mixture was stirred at room temperature for 0.5 h. Concentration under reduced pressure gave an oily residue, which was dissolved in MeCN/DMF/H_2O

(10/9/1, 20 cm^3). Fmoc-OSu (159 mg, 0.472 mmol) and Et_3N (0.094 cm^3, 0.675 mmol) were added to the mixture at 0 °C, and the mixture was stirred at room temperature for 12 h. After being diluted with EtOAc (70 cm^3), the reaction mixture was washed with 1 N HCl and dried over $MgSO_4$. Concentration under reduced pressure followed by flash chromatography over silica gel with *n*-hexane-EtOAc (1:1) gave the title compound **19** (267.3 mg, 65% yield) as a semisolid; $[\alpha]^{24}_D$ −19.6 (*c* 1.13 in DMSO); ν_{max}/cm^{-1} 3333 (OH), 1693 (CO); δ_H (500 MHz; DMSO-d_6) 1.04–1.70 (12H, m), 2.89–3.02 (4H, m), 3.21 (1H, dt, *J* 9.7 and 7.5), 3.98–4.10 (1H, m), 4.22 (1H, t, *J* 6.9), 4.30 (2H, d, *J* 6.9), 4.85 (1H, dd, *J* 37.2 and 9.7), 4.99 (4H, s), 7.19–7.44 (16H, m), 7.65–7.74 (3H, m), 7.89 (2H, d, *J* 7.5), 12.35 (1H, br s); δ_C (125 MHz; DMSO-d_6) 22.6, 23.7, 28.9, 29.0, 30.9, 31.9, 40.0, 40.1, 40.3, 46.6, 51.3 (d, *J* 31.2), 65.0, 65.1, 65.4, 104.0 (d, *J* 12.0), 120.0 (2C), 125.1 (2C), 127.0 (2C), 127.6 (2C), 127.6 (4C), 127.7 (2C), 128.3 (4C), 137.2 (2C), 140.7 (2C), 143.7, 143.8, 155.6, 156.0 (2C), 159.4 (d, *J* 257.9), 174.4; δ_F (470 MHz; DMSO-d_6) −117.9–−118.5 (m); *m/z* (FAB) 766.3512 ([M + H]$^+$, $C_{44}H_{49}FN_3O_8$ requires 766.3504).

General procedure for preparation of peptide by Fmoc-SPPS

The protected peptide chains were constructed on the Novasyn® TGR resin (0.26 mmol g^{-1}, 96 mg, 0.025 mmol). *t*-Bu ester for Asp and Glu; 2,2,4,6,7-pentamethyldihydrobenzofuran-5-sulfonyl (Pbf) for Arg; *t*-Bu for Thr, Tyr and Ser; Boc for Lys; and Trt for Gln, Asn and His were employed for side-chain protection. Fmoc-amino acids (0.075 mmol) were coupled by using *N*,*N*′-diisopropylcarbodiimide (DIC; 0.012 cm^3, 0.075 mmol) and *N*-hydroxybenzotriazole monohydrate (HOBt·H_2O, 11.5 mg, 0.075 mmol) in DMF for 2 h. Coupling of dipeptide isosteres (EADI **10**: 49 mg, 0.063 mmol; FADI **19**, 48 mg, 0.063 mmol) was carried out with DIC and HOBt·H_2O for 12 h. The peptide resins were treated with 1 M TMSBr-thioanisole/TFA in the presence of *m*-cresol and 1,2-ethanedithiol as scavengers. The reaction mixture was precipitated with diethyl ether. The resulting powder was collected by centrifugation and then washed three times with diethyl ether. The crude product was purified by preparative HPLC to afford the expected peptides as a colorless powder. The purity of each compound was assessed analytical RP-HPLC prior to the CD analysis and biological testing (>98%).

Anti-HIV-1 activity

Anti-HIV-1 activity was determined by the multinuclear activation of a galactosidase indicator (MAGI) assay as described previously.[14] Briefly, the MAGI cells (10^4 cells $well^{-1}$) were seeded in flat-bottom 96-well microtitre plates. The following day, the cells were inoculated with HIV-1 (60 MAGI units/well, yielding 60 blue cells after 48 h incubation) and cultured in the presence of various concentrations of peptide inhibitors in fresh medium. After 48 h incubation, all the blue cells stained with 5-bromo-4-chloro-3-indolyl-β-D-galactopyranoside (X-gal) in each well were counted. The activity of inhibitors was determined as the concentration that blocked HIV-1 replication by 50% (50% effective concentration [EC_{50}]).

Measurement of CD spectra

Peptides were incubated at 37 °C for 30 min (the final concentrations of peptides were 10 μM in 5 mM HEPES buffer, pH 7.2). CD spectra were acquired on a Jasco spectropolarimeter (Model J-710, Jasco Inc., Tokyo, Japan) at 25 °C as the average of 8 scans. Thermal unfolding at intervals of 0.5 °C was performed after a 0.25-min equilibration at the desired temperature and an integration time of 1.0 s. The mid point of the thermal unfolding transition (melting temperature, T_m) of each complex was determined from the maximum of the first derivative, with respect to the reciprocal of the temperature, of the $[\theta]_{222}$ values.

Acknowledgements

This work was supported by the Science and Technology Incubation Program in Advanced Regions from Japan Science and Technology Agency, Grant-in-Aids for Scientific Research from MEXT, Japan, and Health and Labour Sciences Research Grants (Research on HIV/AIDS). K.T. and T.N. are grateful for the JSPS Research Fellowships for Young Scientists.

References

1 For review, see: J. M. Davis, L. K. Tsou and A. D. Hamilton, *Chem. Soc. Rev.*, 2007, **36**, 326–334.
2 For recent reviews, see: (*a*) J. Garner and M. M. Harding, *Org. Biomol. Chem.*, 2007, **5**, 3577–3585; (*b*) L. K. Henchey, A. L. Jochim and P. S. Arora, *Curr. Opin. Chem. Biol.*, 2008, **12**, 692–697.
3 T. Matthews, M. Salgo, M. Greenberg, J. Chung, R. DeMasi and D. Bolognesi, *Nat. Rev. Drug Discovery*, 2004, **3**, 215.
4 (*a*) A. Otaka, M. Nakamura, D. Nameki, E. Kodama, S. Uchiyama, S. Nakamura, H. Nakano, H. Tamamura, Y. Kobayashi, M. Matsuoka and N. Fujii, *Angew. Chem., Int. Ed.*, 2002, **41**, 2937; (*b*) S. Oishi, S. Ito, H. Nishikawa, K. Watanabe, M. Tanaka, H. Ohno, K. Izumi, Y. Sakagami, E. Kodama, M. Matsuoka and N. Fujii, *J. Med. Chem.*, 2008, **51**, 388–391; (*c*) H. Nishikawa, S. Nakamura, E. Kodama, S. Ito, K. Kajiwara, K. Izumi, Y. Sakagami, S. Oishi, T. Ohkubo, Y. Kobayashi, A. Otaka, N. Fujii and M. Matsuoka, *Int. J. Biochem. Cell Biol.*, 2009, **41**, 891.
5 (*a*) H. Nishikawa, S. Oishi, M. Fujita, K. Watanabe, R. Tokiwa, H. Ohno, E. Kodama, K. Izumi, K. Kajiwara, T. Naitoh, M. Matsuoka, A. Otaka and N. Fujii, *Bioorg. Med. Chem.*, 2008, **16**, 9184–9187; (*b*) T. Naito, K. Izumi, E. Kodama, Y. Sakagami, K. Kajiwara, H. Nishikawa, K. Watanabe, S. G. Sarafianos, S. Oishi, N. Fujii and M. Matsuoka, *Antimicrob. Agents Chemother.*, 2009, **53**, 1013–1018.
6 Recent applications of alkene dipeptide isosteres: (*a*) C. L. Jenkins, M. M. Vasbinder, S. J. Miller and R. T. Raines, *Org. Lett.*, 2005, **7**, 2619–2622; (*b*) J. Xiao, B. Weisblum and P. Wipf, *J. Am. Chem. Soc.*, 2005, **127**, 5742–5743; (*c*) S. Oishi, K. Miyamoto, A. Niida, M. Yamamoto, K. Ajito, H. Tamamura, A. Otaka, Y. Kuroda, A. Asai and N. Fujii, *Tetrahedron*, 2006, **62**, 1416–1424; (*d*) J. Xiao, B. Weisblum and P. Wipf, *Org. Lett.*, 2006, **8**, 4731–4734; (*e*) N. Dai, X. J. Wang and F. A. Etzkorn, *J. Am. Chem. Soc.*, 2008, **130**, 5396–5397; (*f*) C. E. Jakobsche, G. Peris and S. J. Miller, *Angew. Chem., Int. Ed.*, 2008, **47**, 6707.
7 R. J. Abraham, S. L. R. Ellison, P. Schonholzer and W. A. Thomas, *Tetrahedron*, 1986, **42**, 2101–2110.
8 (*a*) T. Ibuka, K. Nakai, H. Habashita, Y. Hotta, N. Fujii, N. Mimura, Y. Miwa, T. Taga and Y. Yamamoto, *Angew. Chem., Int. Ed. Engl.*, 1994, **33**, 652; (*b*) P. Wipf and P. C. Fritch, *J. Org. Chem.*, 1994, **59**, 4875–4886; (*c*) N. Fujii, K. Nakai, H. Tamamura, A. Otaka, N. Mimura, Y. Miwa, T. Taga, Y. Yamamoto and T. Ibuka, *J. Chem. Soc., Perkin Trans. 1*, 1995, 1359.
9 (*a*) T. Narumi, A. Niida, K. Tomita, S. Oishi, A. Otaka, H. Ohno and N. Fujii, *Chem. Commun.*, 2006, 4720–4722; (*b*) T. Narumi, K. Tomita, E. Inokuchi, K. Kobayashi, S. Oishi, H. Ohno and N. Fujii, *Tetrahedron*, 2008, **64**, 4332–4346.

10 H. Tamamura, A. Omagari, K. Hiramatsu, S. Oishi, H. Habashita, T. Kanamoto, K. Gotoh, N. Yamamoto, H. Nakashima, A. Otaka and N. Fujii, *Bioorg. Med. Chem.*, 2002, **10**, 1417–1426.
11 T. Honda, H. Wakabayashi and K. Kanai, *Chem. Pharm. Bull.*, 2002, **50**, 307–308.
12 H. Sajiki, K. Hattori and K. Hirota, *J. Org. Chem.*, 1998, **63**, 7990–7992.
13 (*a*) D. C. Chan, D. Fass, J. M. Berger and P. S. Kim, *Cell*, 1997, **89**, 263–273; (*b*) D. C. Chan, C. T. Chutkowski and P. S. Kim, *Proc. Natl. Acad. Sci. USA*, 1998, **95**, 15613–15617.
14 (*a*) J. Kimpton and M. Emerman, *J. Virol.*, 1992, **66**, 2232–2239; (*b*) E. I. Kodama, S. Kohgo, K. Kitano, H. Machida, H. Gatanaga, S. Shigeta, M. Matsuoka, H. Ohrui and H. Mitsuya, H., *Antimicrob. Agents Chemother.*, 2001, **45**, 1539–1546.